



# Structure and genesis of the Cubango Megafan in northern Namibia: implications for its hydrogeology

F. Lindenmaier · R. Miller · J. Fenner · G. Christelis ·  
H. G. Dill · T. Himmelsbach · S. Kaufhold · C. Lohe ·  
M. Quinger · F. Schildknecht · G. Symons · A. Walzer ·  
B. van Wyk

**Abstract** An exploration strategy for groundwater was established and followed in the northern Namibian Cuvelai-Etосha Basin (CEB). The data derived from transient electromagnetics, rotary-drilling, coring and sample investigation were used to refine stratigraphy and hydrostratigraphy, and to develop a 3D map of aquifers within the Cubango Megafan. The results have delineated three major aquifers. The newly found, deep-seated Ohangwena II Aquifer (KOH-2) has the potential of providing significant additional water to the water supply of northern Namibia and Angola. While near-surface aquifers carry predominantly brackish water, freshwater in the deep-seated aquifer is further extended and features good hydraulic properties. To date, only a small part of the hydrogeological potential of arid CEB has been explored and an extension of exploration is needed, including southern Angola. The combination of structural, sedimentological and hydrogeological approaches greatly advanced both the geological and hydrogeological understanding. With regard to the deep-seated aquifer, strict measures need to be applied to ensure that the water in the KOH-2 reservoir is exploited sustainably. Water control areas need to be established to ensure long-term preservation of this newly explored aquifer.

**Keywords** Namibia · Conceptual model · Groundwater exploration · Arid regions · Okavango

## Introduction

In its search for potable water, Namibia has embarked on an investigation of the groundwater resources in its part of the Cuvelai-Etосha Basin (CEB), which has a total size of about 160,000 km<sup>2</sup> in north central Namibia near the border with Angola. With both population and economic growth, the demand for potable water is steadily increasing. As most of the near-surface groundwater in the western half of the CEB is brackish to saline, deeper groundwater resources needed to be investigated and tapped. The exploration thereof has been part of joint efforts by Namibian (Department of Water Affairs and Forestry, DWAF) and German (Federal Institute for Geosciences and Natural Resources, BGR) authorities in the Cubango Megafan, a unique palaeo-fluvial system that has supplied sediments to the north-eastern half of the CEB since at least the Miocene (Miller et al. 2010; Fenner 2010; Lindenmaier and Christelis 2012) and that contains freshwater aquifers.

The megafan emerges from the Angolan Highlands in the north and terminates at the north-eastern end of the Etosha Pan (Miller et al. 2010). It can be clearly seen in digital terrain models; however, its geological setup is only marginally known. In order to develop a quantitative interpretation of groundwater resources, a refinement of bio- and lithostratigraphic as well as hydrostratigraphic units that are traceable spatially throughout the megafan is required.

So far, most information available is from the Namibian part of the Cubango Megafan, with about 800 existing groundwater wells in the northern CEB; of these lithologies exist for less than 100. This report presents the results of a basin-wide transient electromagnetic survey as well as successful exploratory drilling for a new deep-seated, freshwater resource. Now, more than 15 boreholes penetrate the full Tertiary to Quaternary Kalahari

---

Received: 20 August 2013 / Accepted: 8 April 2014  
Published online: 4 May 2014

© Springer-Verlag Berlin Heidelberg 2014

---

F. Lindenmaier (✉) · J. Fenner · H. G. Dill · T. Himmelsbach · S. Kaufhold · C. Lohe · M. Quinger · F. Schildknecht · A. Walzer  
Bundesanstalt für Geowissenschaften und Rohstoffe, Stillweg 2,  
30655, Hanover, Germany  
e-mail: falk.lindenmaier@gmx.com

G. Christelis · B. Wyk  
Department of Water Affairs and Forestry,  
Government Office Park, Windhoek, Namibia

R. Miller · G. Symons  
Consulting Geologist, PO Box 11222, Windhoek, Namibia

sedimentary succession (Miller 2008; Miller et al. 2010; Lindenmaier and Christelis 2012). From these results, a first 3D-image of the groundwater system of the Cubango Megafan is drawn, using the software GSI3D.

### Hydrological and geological setting of the Cuvelai-Etosa Basin

The Cuvelai-Etosa Basin (CEB) is a large endorheic hydrological system in the south-west of Africa extending from the southern Angolan Highlands into north-central Namibia (Fig. 1a). It is flanked by catchments of the Kunene and the Okavango in the north. The folded and karsted platform carbonates of the Neoproterozoic Otavi Group form a topographically elevated margin to the south and west of the basin (Fig. 1b). The crest of the Cubango Megafan forms the approximate eastern limit of the CEB.

Annual rainfall is between 400 and 500 mm within the CEB (Mendelsohn et al. 2000) but is up to 1,100 mm at its northern tip in the Angolan highlands (Verissimo 2005), the main headwater catchment of the Kunene, Cuvelai and Okavango River systems. In contrast, annual potential evaporation is estimated at about 2,400 mm (Mendelsohn et al. 2000). Current climate is highly seasonal with a rainy season in December to March and a dry season in April to November. The amount and distribution of rain is highly variable, which is also true in regards to long-term fluctuation.

Topographic gradients are extremely low within the CEB and all drainage systems converge on a common low point, the saline Etosha Pan (Miller et al. 2010). The present day Cuvelai System is a unique hydrological subsystem of shallow interconnected channels of highly variable width, that flood irregularly, combined with headwater catchments in the southern Angolan Highlands. The Cuvelai is divided into the Etaka Catchment in the west and the central Cuvelai Catchment (Miller et al. 2010). The Etaka Catchment only floods when there have been heavy local rains within its areal extent but the Cuvelai Catchment catches precipitation in its elevated main headwater catchments. The flooding of the central Cuvelai Catchment was the main contribution of water for the historically densely populated area. Floods occasionally reach the Etosha Pan when there have been exceptionally heavy rains in the Angolan highlands.

Besides the headwater Cuvelai System, there are remnants of additional drainage systems on top of the former Cubango Megafan (Fig. 2). These south-westerly flowing rivers are most likely remnants of the megafan sedimentation. They are sand-choked, pre-dune palaeochannels which rarely flow, even after heavy rains (Miller et al. 2010). Topographic analysis of a digital terrain model (DTM; METI and NASA 2011) was used to determine the size of potential groundwater feeding areas and to relate these palaeochannels to receiving channels that finally end in the Etosha Pan. It should be noted that the “Oshigambo System” features a larger headwater in

the Angolan Highlands than the “Niipele System” (Fig. 2). There also are some short, shallow, west-flowing rivers which generally arise and end between the dunes, but very few of these join the south-westerly flowing palaeochannels. Numerous small drainage systems in the Otavi and Tsumeb Mountainland complete the hydrological system of the CEB. Parts of the Cuvelai System and Etosha Pan lie below the 1,130 m contour line (hatched area in Fig. 1a). This area, named the Etosha Depression in this report, has the highest abundance of clays in the underlying Kalahari succession (Miller 1997, 2010) and supposedly represents the area covered by a former and much larger Palaeolake Etosha (Buch 1997; Miller et al. 2010).

Left-bank flooding of the low-gradient, south-westerly flowing section of the Palaeo-Kunene River was responsible for the cutting of the myriad shallow, southeast flowing channels of the Cuvelai System up until approximately 4 million years ago (Miller et al. 2010). Subsequent incision by the Kunene River has resulted in the development of a hydrological barrier between it and the Cuvelai System. This barrier is only a few meters in elevation, but is sufficient to prevent even the highest Kunene floods from flowing into the Cuvelai System. Nowadays, water is pumped over this barrier from the Calueque Dam on the Kunene into a channel and pipeline system that provides potable water for the north-western regions of the CEB.

The Owambo Basin is the geological analogy to the hydrological CEB and contains the sediments of the Kalahari Group that govern the hydrogeological system. However, the Owambo Basin extends across the hydrological watershed; compare the extent of Kalahari sediments and the outline of the CEB in Fig. 1a–b. The sediments of the Kalahari Group form the sand-dominated Cenozoic fill in the Owambo Basin. From the base up, these are the red Ombalantu, Beiseb and Olukonda formations and the white Andoni Formation with its green interbedded clay layers. The top of the Andoni Formation consists of a thin layer of white aeolian sands. A field of low, red, vegetated, longitudinal, east-west Kalahari dunes overlies these white sands in the central and eastern parts of the Cubango Megafan. Lunette dunes occur on the western side of Etosha Pan and north of the longitudinal dunes. Low-amplitude, long-wavelength, N–S dunes occur just east of Ruacana and aeolian sand ramps have been built up on the eastern side of dolomite hills (Miller 1997, 2008; Miller et al. 2010). The sandy Andoni Formation in the north has a calcitified age equivalent in the south, the so-called Etosha Calcrete that rims the Otavi Group Carbonates (Fig. 1b).

The Cenozoic sediments of the Kalahari Group house a number of complex and interconnected groundwater systems (Christelis and Struckmeier 2001; Bittner and Kleczar 2006) with possible hydraulic connections to the Kunene and Okavango River systems and beyond. The Cubango Megafan (Stanistreet and McCarthy 1992; Wilkinson et al. 2009) is part of the eastern CEB and the Okavango Basin and features its own specific

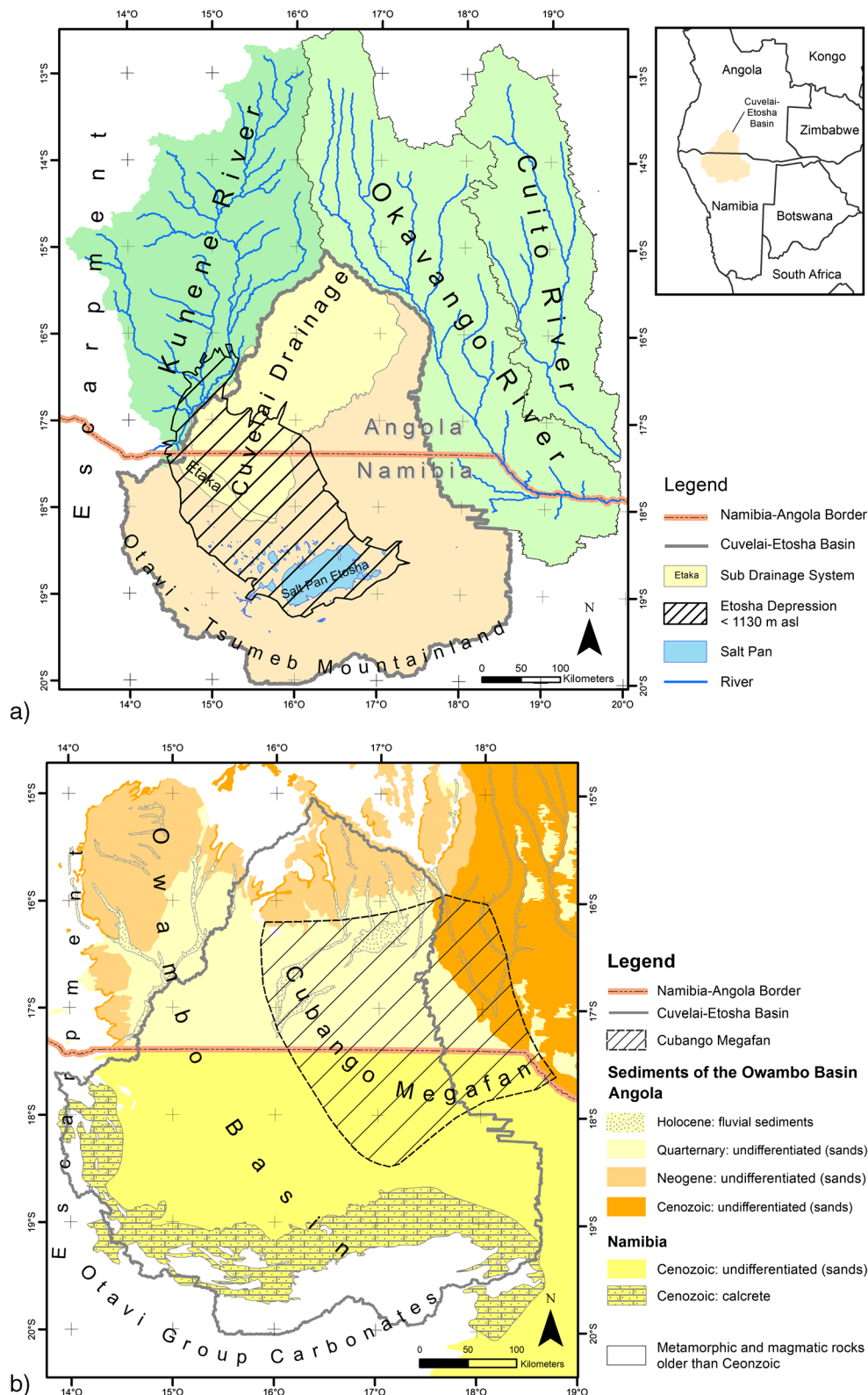


**Fig. 1** **a** Location and outline of the endorheic Cuvelai-Etoshia Basin as well as the upper Kunene, Okavango and Cuito Basins, compiled from ASTER DTM (digital terrain model) data (METI and NASA 2011). The Cuvelai and Etaka sub catchments were delineated from the DTM and data of Mendelsohn et al. (2000). The area below the 1,130 masl contour line is *hatched* and represents the *Etosha Depression* of this study. The inset shows the location of the Cuvelai-Etoshia Basin in southern Africa. **b** Cenozoic sediments of the Owambo Basin and approximate extent of the Cubango Megafan. Sediment distribution is taken from geological maps of Namibia and Angola (de Araújo et al. 1988; Miller and Schalk 1980). In Namibia, Cenozoic calcrete forming an apron along the southern and western margins of the CEB is distinguished from other Cenozoic sediments (Miller 2008; Miller et al. 2010). In Angola, older Cenozoic sediments occur in the north and show evidence of significant amounts of younger erosion

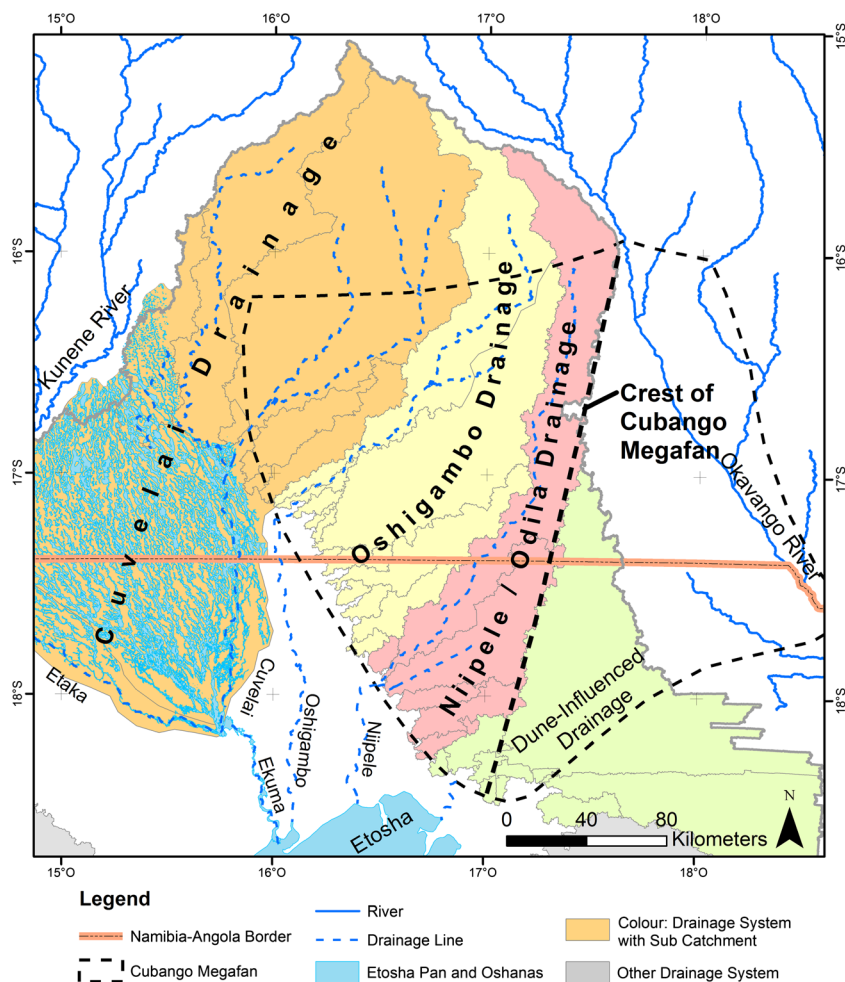


**Fig. 2** Enlargement (Fig. 1b) of drainage systems of the Cuvelai, Niipele and Oshigambo. Contributions from the Oshigambo and Niipele to the Etosha Pan are very minor to negligible. The Cuvelai shows a central part that is flooded

hydrogeological system. It is a former delta of the Okavango River that emerges from the Angolan Highlands. Synonyms of the Okavango are Cubango (in Angola) or Kavango. For clarity in this report, the river is called “Okavango”, while the megafan is called “Cubango”.

### Palaeo drainage systems

Studies of the evolution of the Kalahari basins and their drainage lines (Moore and Larkin 2001; Goudie 2005; Haddon and McCarthy 2005; Miller et al. 2010) show that sediments have accumulated in a relatively flat depression “Kalahari”, that has extended across central southern Africa since the Late Cretaceous. The extremely low gradients within the basins, tectonic movements, and sedimentation by rivers or wind have led to repeated displacements of river systems. The many sharp bends of rivers of central southern Africa like that of the Kunene, that of the Okavango or the Zambezi are the result of river capture which is triggered in part by the afore-mentioned processes and an uplift towards the west. For example, north-west–south-east directed faults formed the flow of Okavango, Cuito, Kwando and Zambezi rivers

(Mendelsohn et al. 2000). Thomas and Shaw (1990) and Moore and Larkin (2001) suggest that the flow line of the Okavango was dominantly south-east from the Late Cretaceous to the Pleistocene. However, a more detailed view to the Upper Okavango reveals a different history for the time between the Miocene and Pleistocene. The DTM reveals that at present time the Okavango clearly cuts the eastern side of its own former deltaic megafan and flows in a SSW direction before it bends to the west at the foot of the megafan. The incision of the Okavango is about 80 m deep where it emerges from the Angolan highlands at the 1,220 masl (meters above sea level) contour line and about 50 m deep at the Angolan-Namibian border. The geological map of Angola (de Araújo et al. 1988) shows that the headwaters of the Okavango are located in metamorphic and plutonic Precambrian rocks; however, there are also mapped remnants of early Kalahari Palaeogene and Neogene sedimentary rocks (Fig. 1b).

Geomorphological interpretations suggest that the Okavango may have stopped flowing during the culmination of aridity. It is also possible that the Okavango may have changed its path when Palaeolake Etosha dried out about 4 million years (Ma) ago (Buch and Trippner 1997; Miller and Schalk 1980). The Oshigambo and Niipele

drainage systems are partly re-activated remnants of that westwards flowing river system (Fig. 2). The beginning of the incision of the Okavango is assumed to start around 1 Ma and postdates the Kalahari dunes as they are very likely cut by the Okavango.

The development of the course of the Palaeo-Kunene River is in debate: The capture of the Kunene by westerly flowing rivers might have happened more than once during the Cenozoic (Buch and Trippner 1997; Moore and Blenkinsop 2002), between 4 Ma to 35,000 years before present (Miller et al. 2010). The Kunene valley is 50 m deep at the 1,200 masl contour line and about 20 m deep near the Calueque Dam (1,100 m). Downstream of the Ruacana Falls, the westerly flowing Kunene River follows through a deep, late Carboniferous valley within which Karoo fluvio-glacial deposits are still preserved (Martin 1950) and cuts the N–S escarpment. Recent investigation of Kalahari sediments suggests an influence of palaeo-Kunene far into the Owambo Basin (Miller et al. 2010; Dill et al. 2012) in the early to middle Cenozoic.

### **The aquifers of the Cubango Megafan**

The Cubango Megafan is one of the most striking but weakly pronounced topographic features in the CEB. The DTM (METI and NASA 2011) reveals a well-shaped curvilinear megafan (Fig. 3a) whose crest has a SSW orientation and serves as a recent water divide. In the south-west, the 1,130 masl contour, located in the centre of the Owambo Basin, forms a step in the Etosha Depression. This is the surface limit of the megafan but the subsurface megafan extends further west, e.g., it is still found in borehole WW201346 (Fig. 3a). The gradient of the megafan is very low; from its apex at the emergence of the Okavango from the Angolan highlands to its toe at the Etosha Pan (Fig. 2), the crest of the megafan loses about 90 m in height over a distance of 250 km that is a slope of about 0.00036. Miller et al. (2010) find a general slope of about 0.00056 but take a different pattern than that used in Fig. 3.

Three aquifers, referred to as the Kalahari Ohangwena Aquifers (KOH), occur in the Cubango Megafan. The uppermost discontinuous perched aquifer (KDP of Bittner and Kleczar 2006) occurs in the aeolian sheets sands, is found throughout the CEB and is named KOH-0. It is an important source for potable water for the local population but yields are limited and little is known about the aquifer; thus, it is not a target for large-scale exploitation. Its spatial and even temporal distribution is closely related to the rainfall as it is fed by direct infiltration.

The upper Ohangwena Aquifer (KOH-1) is said to be located between 60 and 160 mbgl (meters below ground level) in unconsolidated and partially cemented sands (“semi-consolidated sandstones”) of the Andoni Formation (Pielawa et al. 1995; Christelis and Struckmeier 2001; Margane et al. 2005; Bittner and Kleczar 2006). The KOH-1 is confined to semi-confined aquifer system that becomes progressively more brackish as it extends toward the Etosha Depression. The KOH-1 extent is related to the shape of the Cubango Megafan.

It is an important aquifer for decentralized exploitation by means of relatively shallow boreholes with a variety of pump systems. The Rural Water Supply authority of the Ministry of Agriculture, Water and Forestry of Namibia (RWS) drills and maintains most of these boreholes. Particularly during droughts, this aquifer is used as a water supply additional to that of the KOH-0. Yield and quality of water of the KOH-1 is low and very variable, and, as such, it is primarily used for livestock.

Indications of a deep-seated freshwater aquifer—the lower Ohangwena Aquifer (KOH-2)—were first described by Bittner (1998), who drilled a deep borehole (WW37070) for DWAf that reached freshwater at a depth of 190 m. This borehole was the trigger for an exploration program for this new groundwater resource (Schildknecht 2012). Transient electromagnetic soundings (TEM) followed by exploratory drilling have resulted in the successive recognition of the size of this previously unknown aquifer, with the results presented here.

## **Data and methods**

### **TEM sounding**

In 2008, 440 transient electromagnetic soundings (TEM) were conducted (Schildknecht 2012) in order to explore deep-seated fresh groundwater. Soundings are grouped to traverses, the main traverse C spans the Cuvelai-Etosha Basin east–west. Locations of TEM soundings, some of the traverses and boreholes are given in Fig. 4. About 105 of the soundings were within the confines of the Cubango Megafan. A Zonge GDP 16 receiver and coils were used with a 300 × 300 m transmitter loop and frequencies of 1 and 4 Hz. For the evaluation of soundings, the INTERPEX software IX1D was used. During the course of the study, the 4 Hz measurements usually showed a smaller error (Schildknecht 2012). Measurements began near borehole WW37070 (Figs. 3a and 4), the so-called Eenyama school borehole (Bittner 1998), which was 260 m deep and recorded a 23 m freshwater section below a depth of 237 m. Two lags of TEM soundings, oriented around the borehole provided sufficient information for calibration. The resistivities were classified as follows—0–3 Ohm-m: very saline water or clay rich sediment; 3–20 Ohm-m: brackish water; >20 Ohm-m: freshwater. This classification is based on findings in similar environments in north-eastern Namibia (Fielitz et al. 2004). Nodes were added to the resistivity profiles and 2D-vertical profiles were interpolated with the minimum curvature method for a visual supported display within the 3D-mapping software. However, these interpolated sections are only a visual support and should not be used for detailed analysis of resistivity distribution.

### **Recent drilling**

Exploratory boreholes were drilled between 2009 and 2011. The first pair, WW201045 and WW201047, were drilled to a depth of maximum 400 m and provided proof

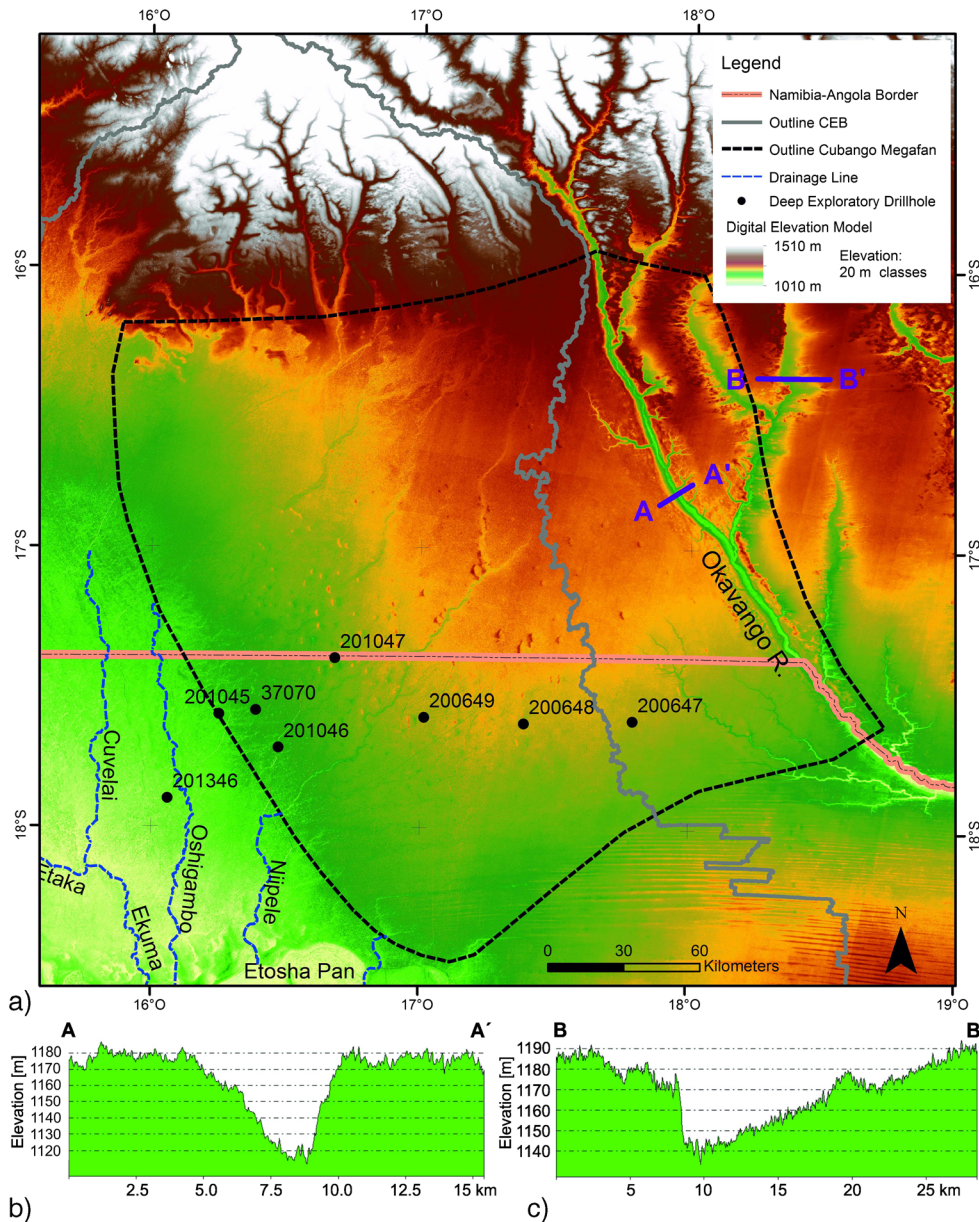


**Fig. 3** a Digital terrain model showing the Cubango Megafan. Locations of key boreholes are shown. **b–c** Cross sections across the Okavango River (*A–A'*; vertical exaggeration 1:60) and a tributary (*B–B'*; vertical exaggeration 1:120) from the DTM; locations of cross sections are shown (a). *CEB* Cuvelai-Etoshia Basin

of the freshwater aquifer KOH-2. Cuttings in WW201045 were taken every 5 m, except for a depth of 246–301 mbgl where material was lost. Also, water quality samples were taken at specific depths and pump tests were conducted. Borehole WW201346 was drilled outside the freshwater area to test the correctness of the TEM soundings; brackish water was expected in KOH-2 and was found.

Coring was done in boreholes WW201216 and WW201217, which were located next to WW201045 and WW201047 respectively. These are the first cored holes drilled into the Cubango Megafan. Coring started at a depth of 80 m and reached depths of 260 and 233 m, respectively.

Undisturbed core sections were retrieved and parts of these sections were analysed for mineralogy, micropaleontology and geochemistry at BGR (Fenner 2010; Dill et al. 2012; Lindenmaier and Christelis 2012; Lindenmaier et al. 2012). For some sections of the core, vertical hydraulic conductivity was determined (Walzer 2010) with a triaxial cell according to the German industry norm DIN 18130 (1998). Cored boreholes WW201216 and WW201217 and rotary boreholes WW201045 and WW201047 are highlighted in this report. Additional boreholes were drilled in 2011 and equipped for monitoring the deep aquifer; lithologs are available but no borehole geophysical logging was carried out.

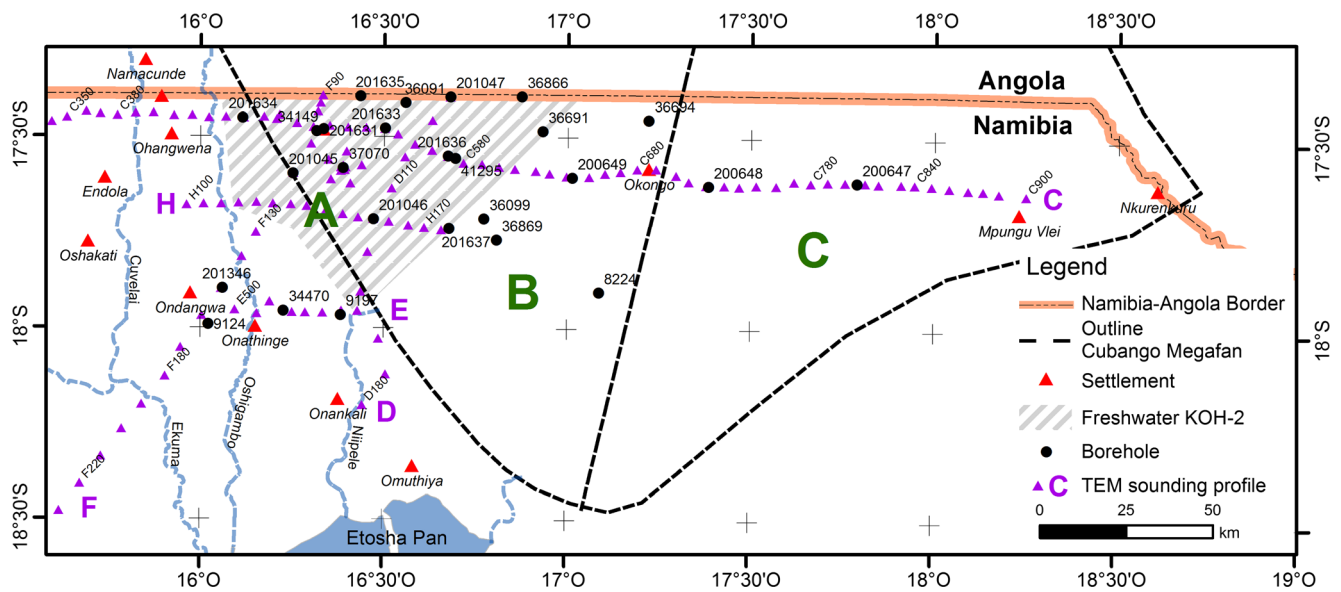


**Fig. 4** TEM sounding locations and traverses as well as relevant boreholes of the Namibian Cubango Megafan. Area *A* is the mapped distribution of freshwater in KOH-2 from the 3D-map. Area *B* lies west of the crest of the megafan and area *C* east of the crest

### Micropalaeontology

Seventeen samples of the core from WW201216 and nine samples of the core from WW201217 were used for micropalaeontological studies. Using heating of a weighted sediment sample with 25 % acetic acid and 30 % H<sub>2</sub>O<sub>2</sub> as well as gravitational separation from clay minerals, concentrates of diatoms and other biosiliceous remains, siliceous remains from land plants (opal phytoliths) and zeolites in the silt fraction were prepared (Fenner 2010; Fenner and DiStefano 2004). The samples were quantitatively analysed by light microscope and examined with the scanning electron microscope. (Fenner and DiStefano 2004; Fenner 2010)

### Geophysical borehole logs

A total of 20 boreholes have been logged with geophysical sounding methods, some from the 2009 drilling campaign and some from previously completed holes. Among other methods, natural gamma ray (GR), apparent resistivity and focused electrical logs (FEL) were recorded as well as magnetic susceptibility (MS). Some boreholes were logged twice. Logs displayed in this report are from different logging campaigns and of variable quality due to old or mal-calibrated systems.

### Historic borehole logs

Records of existing boreholes were digitized and integrated into a lithological database. A reinterpretation on basis of a German standard classification system (Preuss et al. 1991) for all lithologies was conducted. Coordinates of borehole locations are mostly from the national groundwater well database (GROWAS) and are either in Schwarzeck or WGS 1984 geographic coordinates. It is not possible to determine to which of these two systems

the coordinates belong, but displacement between the two systems is about 500 m and this is within the limits of uncertainty of the 3D-map itself. All coordinates were projected to WGS84 UTM zone 33 S for processing with the software GSI3D. The latest boreholes were surveyed recently so that exact coordinates related to survey bench marks exist.

Cuttings from 27 boreholes stored at the Geohydrology Division (GD) of the Department of Water Affairs and Forestry were re-examined and lithologs from several drilling campaigns were included (Bittner 1998, 2008; Van Wyk 2009a, b). Borehole logs were digitized from original borehole reports of the GGD as well as from literature (Miller 2008). Noteworthy are some boreholes from central CEB from the 1960s which were partly cored (P. J. Hugo, Geological Survey South-West Africa, unpublished report, 1969) in Miller (2008). Data from a total of 94 boreholes were incorporated into the study.

### Surface topography

Rastered digital terrain data (DTM) from the most recent ASTER GDEM (Global Digital Elevation Map) release were used (METI and NASA 2011) as the basis for analysis and 3D-mapping. Hydrological watershed delineation was conducted for the CEB, and the Kunene and Okavango basins. The surface-water drainage lines of CEB rivers, and the Kunene and Okavango rivers were determined; elevation information for boreholes was also derived from this DTM. Roads, elevated in reality, are in some cases displayed as valleys on the DTM, with a depth of about 15–20 m. This is approximately the height of the trees in the forest covering the Cubango Megafan, which suggests that the ASTER GDEM displays in some parts the top of the forest canopy and not the land surface. That means that actual boundaries and planes of the 3D-map

may be shifted because the boreholes are attached to the DTM within GSI3D. This is a systematic error that has to be considered when exact elevations are needed, but most of the used logs did not have reliable height information anyway. All elevations above sea level mentioned in this text are related to the ASTER DTM.

### **Geological maps and cross sections**

The geological map of Namibia at 1:1,000,000 scale (Miller and Schalk 1980) was available in digital format; however, differentiation of the Cenozoic, including the Kalahari sequence, is rough and distinguishes only two lithological units. In addition to this, the geological map of Angola at 1:1,000,000 scale (de Araújo et al. 1988) was partly digitized by BGR and contains a more diverse differentiation of the Cenozoic. Both maps contained contours of the base of the Kalahari Formation that fit together quite well, but give no source information. A figure of Miller (2008) and a map of Haddon (2005) and Haddon and McCarthy (2005) show a slightly different depth distribution but seem to be based on the same source, so that the oldest information was taken. The shape of the base of the Kalahari Formation as it evolves from the combination of both maps is of an endorheic system with no outflow. To the authors this does not seem to be plausible, but more detailed information can only be derived through additional investigation and geophysical soundings. Cross sections from Miller (2008) were used to support 3D-mapping.

### **Three-dimensional mapping with GSI3D**

To combine information from all sources, the 3D-mapping software GSI3D was used (Mathers et al. 2011; Sobisch 2014). It combines the construction of 2D cross-sections with a mapping tool. 3D-volumes of bodies are then calculated from the 2D horizontal and vertical information. The quality of information required a hierarchical approach. Lithofacies units delineated by Dill et al. (2012) were identified on geophysical logs. A first network of 2D vertical sections was created. Units were then connected to each other from borehole to borehole. Correlation of lithofacies units and geophysical logs seemed to work exceedingly well, even over distances of more than 50 km between boreholes. Not all lithofacies units have a megafan-wide distribution and lithofacies change from distal to proximal and from west to east.

Additional deep boreholes lacking geophysical logs were included into the network. The detailed lithological descriptions were used to identify possible similar lithofacies. The first network had priority over this second network. TEM soundings were also included. Classified resistivity logs were given a higher priority to interpolated sections. TEM soundings were used to draw an approximate boundary between fresh and brackish water.

## **Results**

The 3D-structure mapping of the extent of lithostratigraphic and hydrogeological layers within the Cubango Megafan is a challenging task due to the sparse data density both in lateral and vertical directions. The only outcrops of older Kalahari sediments are in the northern CEB in Angola (Fig. 1b) and the available information thereon was incorporated to help understand the system and to make future recommendations on water exploitation and management. A hydrogeological regionalization is the aim of this report and is based on present knowledge about stratigraphy, lithostratigraphy and paleontological setting of the Cubango Megafan and its correlation to other sedimentary units within the CEB; compare Miller et al. (2010) and Dill et al. (2012) who provide more detailed information than is given here.

### **Thickness of the Kalahari succession in the CEB**

The thickest Kalahari section of 462 m above pre-Kalahari basement in the CEB was encountered in borehole WW9124 near Olukonda Mission (P. J. Hugo, Geological Survey South-West Africa, unpublished report, 1969; Miller 2008). Borehole WW201045 was stopped at a depth of 400 m, when a significant increase of drill pressure head and decrease of drill progress suggested that the Olukonda Formation had been reached.

Hedberg (1979) suggests that the pre-Kalahari floor of the basin deepens to 600 mbgl toward the Angolan border; however, interpretation of seismic data from a vibroseismic survey for Etosha Petroleum Ltd. (Hedberg 1979) was not possible due to breaks in the reflection. Hedberg's isopachs are based solely on borehole interpretation and data from boreholes north of WW9124 did not exist at this time.

Haddon (2005) and Haddon and McCarthy (2005) show a drainage system in the pre-Kalahari basement arising south of the Otavi Mountainland, flowing northeast around the eastern side of the mountainland and then flowing northwest into the CEB. There are no borehole data to indicate where or even whether this drainage system exited the basin but an exit may have existed to the north-east (Miller 2008) such that this Cretaceous to Late Cretaceous valley system may have joined south-easterly flowing rivers (earliest Okavango) that were tributaries to a palaeo Limpopo River. Miller (2008) has suggested that the basal Kalahari sediments in the CEB could be Late Cretaceous in age.

The geological map of Angola (de Araújo et al. 1988) postdates the geological map of Namibia (Miller and Schalk 1980). Isopachs of the bottom of the Kalahari Basin of both maps fit together so that it is assumed that isopachs of the Angolan map were constructed according to the Namibian map (Fig. 5). It is not known whether any borehole logs or geophysical survey underlie these isopachs. However, when isopachs are combined from both maps, the shape of an endorheic basin that postdates the evolution of the Kalahari sedimentation is drawn (Fig. 5).



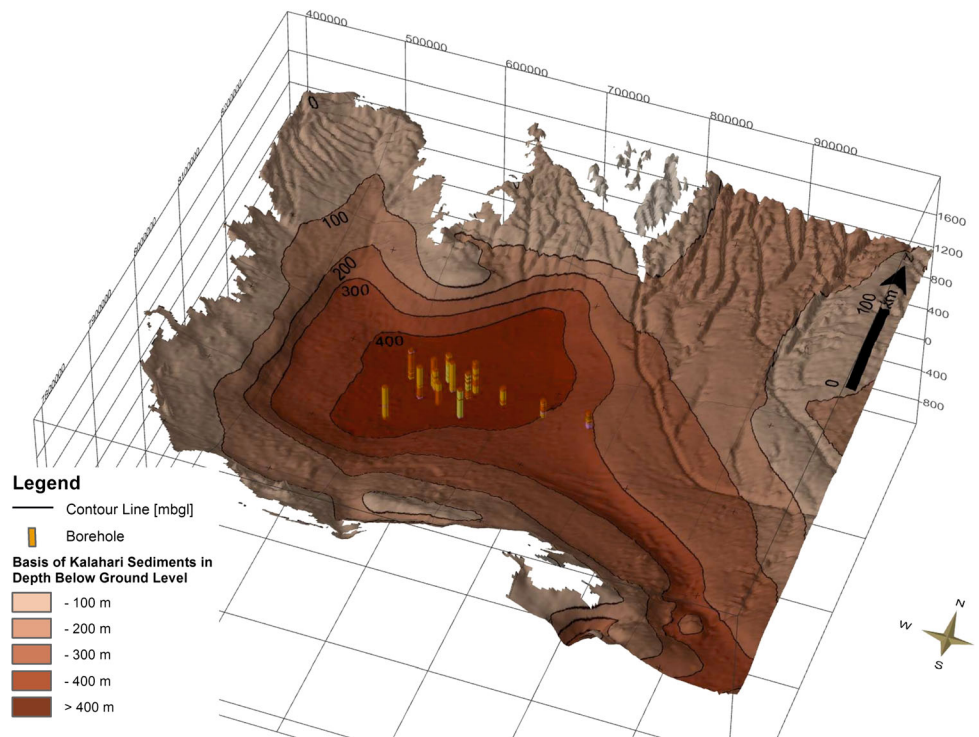


**Fig. 5** Information derived from the geological maps of Angola and Namibia. View is exaggerated 100 times: a 3D-display of the pre-Kalahari floor of the Owambo Basin with a depression in the centre of the basin and a channel-like structure entering from the south-east. Contours are depth in meters from the current surface (ASTER DTM)

An inconsistency in interpretation and data of the pre-Kalahari drainage evolution (Miller 2008; Haddon 2005; Haddon and McCarthy 2005) and the shape of the Kalahari-Basis as it is found in the two geological maps (de Araújo et al. 1988; Miller and Schalk 1980) is assumed. A “no-outlet” as the maps indicate contradicts the assumed pre-Kalahari drainage pattern and the erosional character of pre-Kalahari sediments that were recovered in the deep boreholes (Miller 2008). After all, tectonic activity, which has not been used for interpretation so far is a process that needs to be considered; hence, isopachs need to be revised. The base of the Kalahari sediments is a hydrogeologically important boundary and a seismic Angolan-Namibian survey, or a deep-seated helicopter TEM, would greatly enhance the information of the hydrogeological systems of the CEB.

### Lithofacies units as hydrogeological markers

Geologic evidence suggests that Kalahari sedimentation in the Owambo Basin began in the Late Cretaceous to early Palaeogene (Miller 2008; Miller et al. 2010). The formations in the CEB (Miller 2008; Table 1) are known only from cuttings and cores of boreholes and are typical for a sedimentary fan (Miller et al. 2010). Lithofacies units (LU) change laterally from basin centre to the rim (Dill et al. 2012). No explicit chronostratigraphic markers have been identified, which makes it difficult to draw final conclusions about the sedimentary development.

The borehole WW201045 (and nearby cored borehole WW201216) is so far the best investigated site on the

western rim of the CEB (Dill et al. 2012). It gives a detailed overview of the hydrographic and hydraulic evolution. Definition of the lithofacies units (Table 1) is based on the combination of grain size variation, chemical composition logs of  $\text{SiO}_2$ ,  $\text{Al}_2\text{O}_3$  and  $\text{K}_2\text{O}$  and geophysical logs (Dill et al. 2012). In addition to this, the investigation of heavy, light and clay minerals support this division which also correlates with palaeo-hydraulic regimes.

Cementation types were identified and used to discuss palaeo-hydroenvironments. The results give an idea about the spatial and temporal evolution of the sediments (Fig. 6) and help to identify the hydrogeological system within the basin (Dill et al. 2012). One unit that is not described by Dill et al. (2012) occurs on top of these lithofacies units and represents Pleistocene sediments that are described by Buch and Trippner (1997) and Miller et al. (2010). The following gives a summary of lithofacies units at site location WW201045/WW201216 and advances the description of Dill et al. (2012) with hydrogeological aspects.

- Lithofacies Ia (<400–350 mbgl). Gamma and FEL conductivity logs are elevated in relation to LU Ib (Fig. 6). This is partly due to elevated clay content (lower part that is described as silty clay in the litholog) but also elevated detrital input (upper part of LU Ia). The overall detrital input is decreasing upwards which is indicated by decreasing Zr and Ti content, except for the top of the section (350–360 mbgl) which shows a Zr-peak. LU Ia is described as a

**Table 1** Relation of stratigraphy, lithofacies units and hydrostratigraphy within the Cubango Megafan as well as mean hydraulic conductivity values derived from tri-axial flow tests on undisturbed core sections (one value for each tested section). Definition of lithofacies units is based on the combination of the investigation of heavy, light and clay minerals plus geochemical and geophysical logging

Formation	Lithofacies units	Hydrostratigraphy	Hydraulic conductivity, WW201045/WW201216 [m/s]	Hydraulic conductivity, WW201047/WW201217 [m/s]	
Upper Andoni	VIII	KOH-0 (KDP) Aquifer	–	–	
	VII	Aquitard and secondary aquifer	–	–	
	VI	KOH-1 Aquifer and secondary aquitard	–	$2.2 \times 10^{-07}$	
	V	KOH-1 Aquifer and secondary aquitard	$4.0 \times 10^{-10}$	$6.3 \times 10^{-08}$	
				$1.1 \times 10^{-06}$	
Lower Andoni	IV	Aquitard	$1.2 \times 10^{-11}$	$9.1 \times 10^{-12}$	
				$2.9 \times 10^{-11}$	
	III	Aquitard	$1.4 \times 10^{-12}$	$4.1 \times 10^{-12}$	
				$5.9 \times 10^{-12}$	
Olukonda	II	KOH-2 Aquifer	$1.1 \times 10^{-09}$	$6.0 \times 10^{-06}$	
					$3.3 \times 10^{-09}$
					$4.9 \times 10^{-08}$
					–
Beiseb (top), Ombalantu (bottom)	Ib	KOH-2 Aquifer	–	–	
	Ia	Aquitard	–	–	
Single well pump test in LU II and Ib			$1.8 \times 10^{-05}$	$1.3 \times 10^{-05}$	

proximal alluvial fan plain deposit with fluvial channels that prograde towards the basin depression (Dill et al. 2012). According to the cuttings, a poorly sorted fine-medium grained sand with silt is encountered. The grains are sub-angular to well rounded. The sediment can be cemented by silcrete or calcrete, which is red in colour. Characteristic are rare large sub-angular quartz grains within a finer grained matrix.

- Lithofacies Ib (350–300 mbgl). Low gamma ray and conductivity paired with low Zr and Ti content, as well as elevated SiO<sub>2</sub> characterise this LU. Fluvial deposits seem to give way for more alluvial deposits. The grain-size distribution is different to the lower part of LU Ia with less fine-grained components and stable distributions of sand-sized grain portions. The colour varies from red, light red to pink with white calcretes in between. A low electrical conductivity relates to freshwater within this LU. The change of lithofacies in between LU Ia and LU Ib is taken as the lower boundary of the aquifer KOH-2.
- Lithofacies II (300–233 mbgl). This facies shows continuous low gamma and conductivity values, with two characteristic peaks of gamma ray; the upper one, 270 m deep, could relate to a calcrete layer, as a calcite-rich sample was retrieved at this position. The sands of LU II are uncemented and coring below 260 mbgl became impossible. White, grey to light-red dominantly fine-grained sands are present, with good sorting while the rare large grains diminish. Calcrete and dolocrete nodules are found within this LU. In general, sample retrieval both for the rotary as well as the core drill lack material and so interpretation is more difficult in this section. According to Dill et al. (2012), LU II is characterized by regressive fluvial

deposits but includes perennial wet lake margin mud-flat facies. An important hiatus ends this fining-upwards sequence. LU II represents the upper part of the aquifer KOH-2.

LU Ia forms the uppermost part of the Ombalantu Formation, the Beiseb Formation (Miller 2008) being either absent or represented by the coarse detrital top of LU Ia. LU Ib and II belong to the Olukonda Formation as described by Margane et al. (2005) and Bittner and Kleczar (2006). Miller (2008) first described the formation for WW9197 which is located at a similar radial position as WW201045 on the megafan.

The term “mud flat” of Dill et al. (2012) refers in this case to the recent Okavango delta (McCarthy et al. 1986) where seasonal flooding and sedimentological and biological processes combine to produce a unique depositional environment. Sediments deposited there are mainly of fluvial and aeolian particulate origin with low-concentration solutes in the water. Bed load (sand fraction) and minor suspended load (clay mineral fraction) transport dominate the fluvial system (McCarthy et al. 1991; Milzow 2008; Milzow et al. 2009). Transport processes influence the deposition of the respective material (Garstang et al. 1989), e.g. sand is deposited in the channels and calcrete/silcrete and halite in places where water evaporates (Milzow 2008). Removal of material within such a system is governed by aeolian sediment transport during dry seasons following spontaneous combustion fires where reed beds and papyrus have died off after channels become clogged up. LU II might present such a fluvial system adjoining to a lake. The lack of clay-sized particles in the sediments is attributed to the lack of those in the river flow.

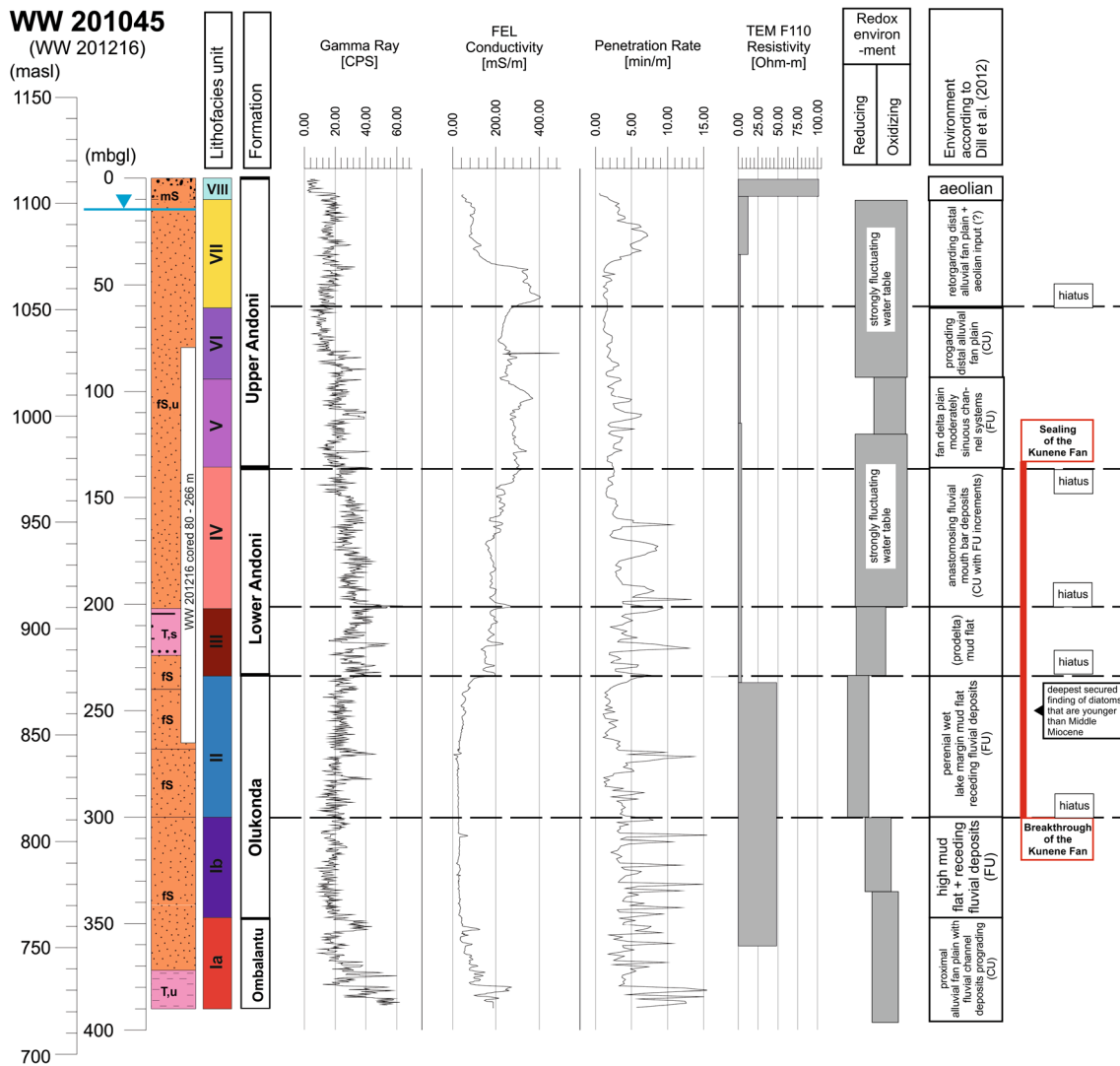


**Fig. 6** Borehole *WW201045*: litholog from interpretation of drill cuttings; gamma and conductivity logs were taken in the open borehole. The penetration is recorded by hand during drilling; it indicates where cemented layers (calcrete or silcrete) were intersected. The section from 10 to 40 m below ground level (mbgl) is a so-called “sticky matrix” that is encountered throughout the megafan but whose composition is still unclear. TEM sounding *F110*, which is located near the borehole, is also recorded and shows a good relationship to the gamma and conductivity logs. The redox environment column shows approximate hydrochemical conditions during deposition derived from mineral and cement analyses (based on descriptions by Dill et al. (2012))

- Lithofacies III (233–200 mbgl). This marks the beginning of the progradation of the megafan series (Dill et al. 2012). The gamma ray signals of the borehole logs have maximum values (Fig. 6). The electrical conductivity signal shows a succession of peaks that are traceable to adjacent deep logs. Often, this unit is described as a red sandy-clay in lithologs; however, the core reveals grey fine-grained sands with purple patches and increased clay contents and calcrete as well as dolocrete nodules. Burrows of animals and plant roots are responsible for the purple patches. From LU II upwards, parts of the core are well cemented and could also be described as sandstone. Two aspects derived from the cores are noteworthy: (1) the amount of thin, interbedded clay-rich layers increases; (2) the general content of clay in sand layers increases. However, these changes seem not to be so significant that LU III is well documented in all lithologs. In drill cuttings, this lithological change seems not to be found in every borehole. This implies that this may not be a continuous layer or it has gone unnoticed during logging of some boreholes. Dill et al. (2012) describes the sedimentological environment as interfingering of lacustrine mud flats with ephemeral lacustrine deposits, with a saline lake adjacent to WW201346. LU III is a potential marker horizon and forms the base of the Andoni Formation.
- Lithofacies IV (200–135 mbgl). This is made up of sediments of a low-gradient fan with alternating anastomosing and meandering fluvial deposits (Dill et al. 2012). The gamma ray signatures are slightly less elevated than in LU III but stay on a high level; the FEL conductivity log is slightly increasing upwards. The SiO<sub>2</sub> content is increasing continuously with

periodic interruptions. LU III and IV form the lower part of the Andoni Formation. The higher abundance of clays relative to higher up in the section (Fig. 6) suggest that the Palaeo-Kunene, which appears to have been more clay rich than the Palaeo-Okavango, may have contributed some of the sediments to this unit. The influence of the Palaeo-Kunene seems to have been significantly less above LU IV. The sediments are grey to purple fine-grained sands with silt and clay (“clayey sands”). Patches of purple indicate animal burrows.

- Lithofacies V (135–95 mbgl). This marks the onset of deposition of the Upper Andoni Formation which accumulated in a fan delta plain with seasonally wet swamps (Dill et al. 2012), i.e. similar to the Okavango system as described by McCarthy et al. (1991). However, it features only minor hydraulically relevant layers like those in LU Ib and II, some of which are aquifers. Hence, LU V is part of KOH-1 system. The gamma ray signature is again slightly less elevated than in LU IV. Light grey, fine-grained sands with varying portion of silt and clay and some calcrete nodules characterise this LU.
- Lithofacies VI (95–60 mbgl). This was deposited under more humid conditions with increased runoff on a prograding distal alluvial fan plain (Dill et al. 2012). These sediments contain major parts of the aquifer KOH-1 in borehole WW201045. The gamma ray log shows slightly decreased values in relation to LU V but elevated conductivity signals. The chemical trends are continued from LU V. The lithological difference to LU V is not so great; the grey to yellow silty sand also shows aeolian influence but is still of fluvial origin.
- Lithofacies VII (60–10 mbgl). This is interpreted as a retrograding distal alluvial fan plain succession within which an aeolian component is incorporated. Aeolian grains become ever more abundant upwards in the succession (Miller et al. 2010; Dill et al. 2012; Miller 2013) and attest to semi-arid climatic conditions that became ever more arid climate with time (Dill et al. 2012). The top of this unit provides the last evidence of fluvial conditions in the Cubango Megafan prior to formation of the Kalahari dune systems. This supports evidence that Palaeolake Etosha gradually shrank to a fraction of its original size and finally dried up completely shortly after 4 Ma ago (Miller et al. 2010). These white to yellow sands have a higher aeolian component; finer grained sediments and calcretes are reduced to the lower part of this LU.
- Lithofacies VIII (10–0 mbgl). This is a white, generally well sorted, aeolian sheet sand containing abundant highly spherical quartz grains. The layer must be later than megafan accumulation (<4 Ma), but immediately precedes the culmination of the arid conditions during which the Kalahari dune systems formed (3–2 Ma) in this region and in the rest of the central and southern Kalahari Basin (Miller et al. 2010). The red Kalahari dunes in this region overlie

this unit and are in marked contrast to it colour-wise. LU VIII contains the KOH-0 Aquifer.

### **Micropalaeontology**

A micropalaeontological investigation of undisturbed core sections of lithofacies units II–VI (Fenner 2010) revealed siliceous remnants of land plants (phytoliths) and siliceous skeletal remains of aquatic organisms: algae (diatoms) and spicules of sponges. The siliceous remnants of the algae are valves of freshwater benthic, planktonic and tycho-planktonic diatoms and resting spores of *Chrysophyceae*. Of these, phytoliths are the most abundant remains and were found in all samples. Most abundant are phytoliths of C4-grasses which dominate in tropical and subtropical regions with low to moderate soil moisture.

The occurrence of one single specimen of the planktonic diatom genus *Aulacosira* is an indication of a deeper lake environment. Another specimen is characteristic for weakly alkaline saline lakes (*Cyclotella meneghiniana*, Hecky and Kilham (1973), which was found in WW201217 at a depth of 105.05 mbgl (Fenner 2010). Samples from WW201216 have characteristics of a slightly wetter environment than those from WW201217 which is also more proximal on the Cubango Megafan. Normally, clay-rich layers have a higher fossil content than sandy layers. The reverse is the case in the two cored boreholes of the Cubango Megafan due to stronger silica diagenesis in the clay layers. The dominance of remains of C4-grasses together with the occurrence of diatoms of the genus *Cyclotella* (Fig. 6) suggests that the age of the deposits lies somewhere in the time interval from middle Miocene to Recent (Fenner 2010).

### **Hydrostratigraphy and hydraulic parameters**

#### *Ombalantu Aquitard*

The Ombalantu Formation (LU Ia) is seen as the hydraulic base of the KOH-2 Aquifer. Elevated gamma ray and FEL conductivity values characterize this unit. The complete formation was penetrated in old exploratory boreholes (Hedberg 1979; Miller 2008; P. J. Hugo, Geological Survey South-West Africa, unpublished report, 1969) but was only reached in this project in boreholes WW201045, WW201047 and WW201346; thus, borehole-based 3D-mapping of LU Ia is not possible. However, the west-east TEM profile C (Fig. 8) gives indirect evidence of a doming up of this formation between Okongo and Mpungu Vlei, which parallels the shape of the base of the Kalahari.

#### *KOH-2 Aquifer*

The KOH-2 Aquifer is represented by LU Ib and LU II. TEM sounding F110 directly next to WW201045 coincides well with the FEL conductivity profile (Fig. 6). The aquifer consists of fine-to-medium-grained sand, often

with a light to darker red or grey colour. Well-sorted sand with well-rounded grains dominates. In LU II, some clay is present, whereas LU Ib is almost clay free; however, there are layers cemented by calcrete and silcrete. For the rest, cementation is very weak. REM images reveal that the sand usually contains only traces of clay, e.g. at a depth of 199 mbgl in WW201047 (Fig. 7c). The thickness of the aquifer is 117 m in WW201045. Single well pump tests with flow rates of about 16 m<sup>3</sup>/h give an average hydraulic conductivity of  $1.8 \times 10^{-5}$  m/s for WW201045 (Table 1); the water table lies at ~15 mbgl for KOH-2.

#### Lower Andoni aquitards

The confining unit on top of KOH-2 is formed by LU IV and LU III. Characteristic are elevated clay contents and a low hydraulic conductivity. Layers are both fining and coarsening upwards (Dill et al. 2012). Grain-size distribution varies from sandy clay (>50 % clay) via fine clayey sand (~20 % clay sized particles) to sand with less than 10 % of clay-sized particles. The sands are pale yellow but have been discoloured by two periods of bioturbation, e.g.

by roots and burrows that produced a grey colouration initially and then a red colouration subsequently. REM images reveal that hydraulic conductivity is determined both by the amount of clay-sized particles as well as by authigenic clay minerals that have grown in pore spaces. In some cases, remnants of a smectite gel are found (Fig. 7). An amount of 20 % or less of fines can reduce the hydraulic conductivity significantly. Gamma ray logs and grain-size distribution derived from cutting samples do not completely reveal such a hydraulic barrier, which complicates the identification of aquifers and aquitards in the lithologs or during the drilling process. Hydraulic conductivity of undisturbed core sections of WW201216 was determined using triaxial cells. Tests for sections of LU V to LU II showed values of  $9 \times 10^{-08}$  to  $7 \times 10^{-13}$  m/s (Table 1), whereas LU III showed the lowest values. Core sections of LU VI to LU II for WW201217 were also examined and values of  $6.0 \times 10^{-06}$  to  $4.1 \times 10^{-12}$  m/s were obtained (Table 1). A vertical hydraulic conductivity of  $6 \times 10^{-6}$  m/s in LU II in WW201217 agrees well with results of the general hydraulic conductivity ( $1.3 \times 10^{-5}$  m/s) for the single well pump tests in adjacent borehole WW201047.

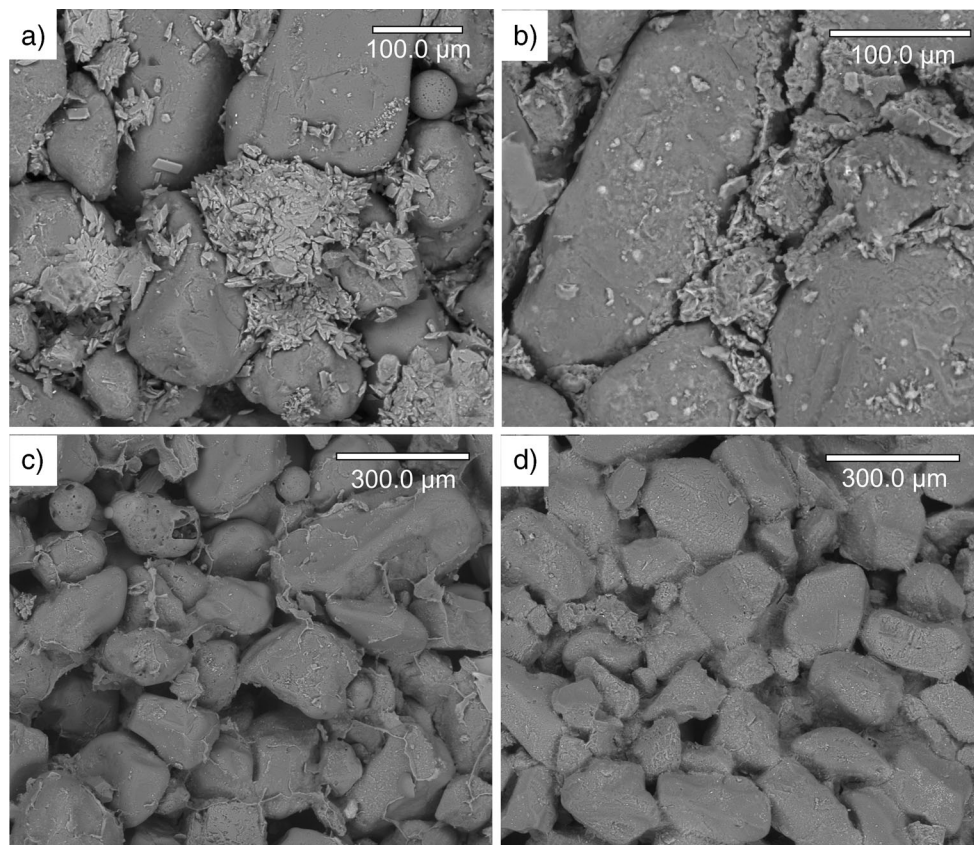


**Fig. 7** REM images of undisturbed core sections provide an impression of the distribution of clay and sand-sized particles. Relatively homogenous sections were selected for hydraulic conductivity determination (see also Table 1) and REM images. Core borehole WW201217 is located next to WW201047 and core borehole WW201016 next to WW201045. **a** WW201217, depth 89.9 m, quartz grains, clinoptilolite and carbonate, vertical hydraulic conductivity  $2.2 \times 10^{-7}$  m/s; **b** WW201217, depth 126.43 m, quartz grains and clay minerals, vertical hydraulic conductivity  $2.9 \times 10^{-11}$  m/s; **c** WW201217, depth 199.6 m, quartz grains and clay mineral coating (smectite), probably remnant of a smectite gel, vertical hydraulic conductivity not available; **d** WW201216, depth 249 m, quartz grains with clay coating (smectite), vertical hydraulic conductivity  $3.3 \times 10^{-9}$  m/s. Images also show spherules of “DryFlo” that were used to determine porosity (a and c)

### KOH-1 Aquifer

The aquifer KOH-1 lies within LU V and VI. In WW201045 it is filled with brackish water, whereas in WW201047 it contains freshwater. The water table in a borehole near WW201045 lies at ~37 mbgl for KOH-1. KOH-1 is the dominant groundwater resource for water supply at elevations approximately above 1,150 masl, the approximate saltwater–freshwater boundary, but many boreholes only have low yields. Standard borehole depth is 150 m for recent boreholes drilled on behalf of Rural Water Supply (Van Wyk 2009b) and those drilled for the Ministry of Lands and Resettlement (Miller 2010). These boreholes have good lithologs and cover LU VIII to LU III; however, these lithologs show a very high lithological heterogeneity with stacked layers of sands, clayey sands, calcretes and clays. This lithological heterogeneity hinders lateral correlation between boreholes and complicates the interpretation of the lithology in terms of regional lithofacies units. No geophysical logging was conducted in these boreholes.

Three boreholes with geophysical logs (WW200647–WW200649, Fig. 10) located up to 80 km apart in an east–west direction (Fig. 8) show comparable sections, suggesting that geophysical borehole logs would give more precise information about lateral lithostratigraphic or hydrostratigraphic changes. In addition, TEM soundings show a decrease in water salinity east of C580. The resistivity values increase and high resistivities are found from ground level down to the Olukonda Formation (Fig. 8). This contrasts with the layered resistivities west of C580. However, this means that the resolution of TEM soundings in the east does not differentiate between aquitards and aquifers.

### Upper Andoni Aquitard

The KOH-1 Aquifer is capped by the confining properties of LU VI and VII. In some parts of the Cubango Megafan, KOH-1 might not be confined or is only partly confined;

however, in most parts it is confined (Van Wyk 2009b). The aquifer consists of fine-grained sands with varying silt and clay contents. Remarkable is a so-called “sticky matrix” that is approximately found from 10 to 60 mbgl. No sample of this sticky matrix could be examined so far in the laboratory but Van Wyk (2009a) reports that (1) the “stickiness” decreases when the sample dries, (2) the section has a considerable resistance while drilling, and (3) it is confining; and, additionally, it is described in the boreholes drilled during this campaign as well as in numerous boreholes from the Rural Water Supply drilling campaigns (Van Wyk 2009b); note the penetration rate in the log in Fig. 6 from a depth of 10–50 mbgl. Also, it is assumed that smectite gels or silicate gels are the reason for this “sticky matrix”; and, in some areas, calcretes produce confining sections within the LUs.

### KOH-0 Aquifer

The KOH-0 Aquifer (variously referred to as “perched aquifer” or KDP) lies on the aquitard of LU VII. The aquifer sands are largely fine-to-medium grained, with only very minor silt. Sorting is reasonably good and grains are mainly well rounded. It is predominantly a white, non-calcareous to slightly calcareous sand, while the uppermost 1–2 m is brown in places and a reddish, 2–4-m-thick zone, typical of soil profiles, may be present some 4 m below surface. The thickness of this aquifer ranges from 1 to 40 m according to borehole logs (Miller 2013). The 3D-map gives a median depth of 13.6 m and an average depth of 13.4 m; and, whereas maximal thickness is 34.8 m, the 25 and 75 quartiles lie at 10.4 and 16.6 m, respectively.

A broad-leaf forest that covers the region on the Cubango Megafan is related to specific depths of the KOH-0 Aquifer (Fig. 9). In the far eastern part of the area where the broad-leaf forest becomes patchy, aeolian sand of the aquifer is still present but the vegetation consists of a mosaic of small treeless grassy patches interspersed with patches of forest in which acacia thorn can be dominant.

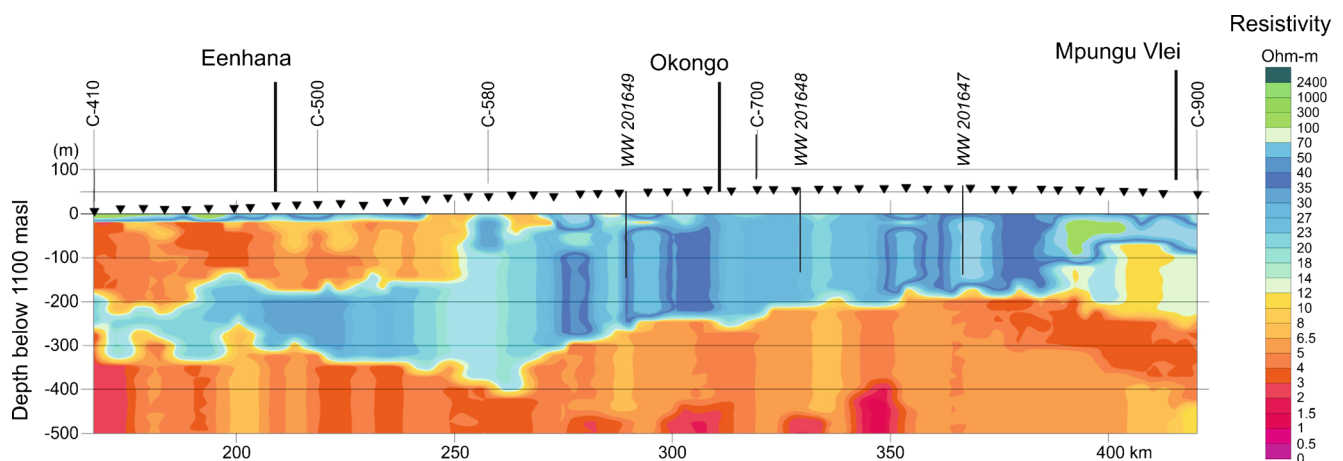


**Fig. 8** Interpolation of TEM soundings of traverse C (based on Schildknecht 2012; see Fig. 4 for location). A significant change in resistivity occurs east of sounding C580, where the water column seems to be fresh throughout. Borehole logs, however, also show saline layers which are not resolved by the TEM sounding. West of C580, there is a low-resistivity layer with higher salinity and clay content at the top of the succession

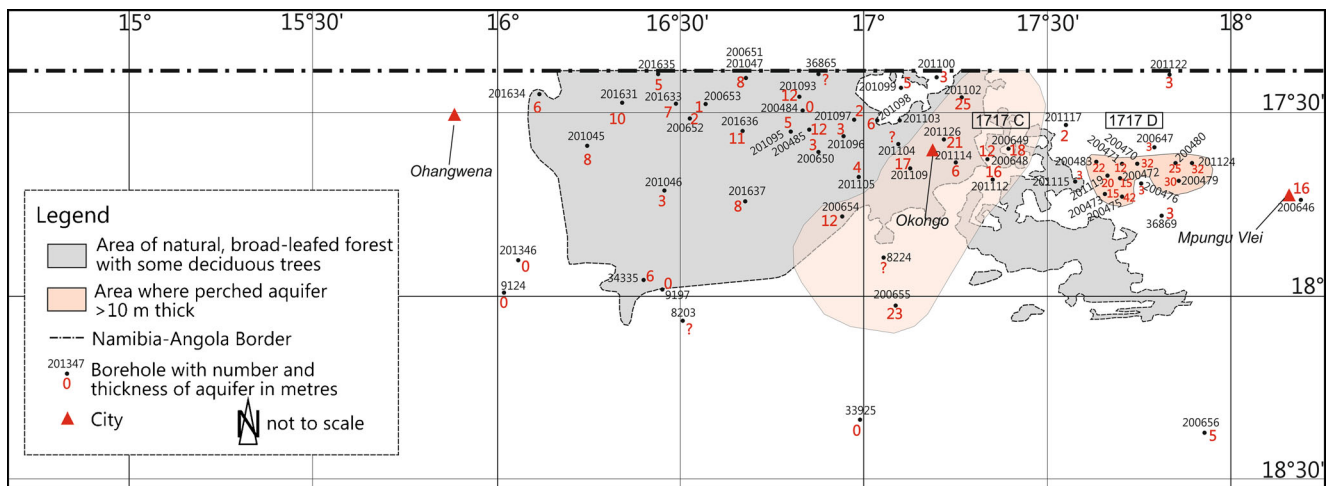


**Fig. 9** Map of the thickness of the KOH-0 Aquifer in boreholes (Miller 2013). Broad-leafed forest is sustained by the aquifer where it is shallow but is absent where the aquifer becomes too deep (pink areas or parts thereof)

West of  $16^{\circ} 10' E$  are grassy plains, shallow channels and vleis that typify the Cuvelai drainage system. The KOH-0 is absent, and highly saline calcrete underlies a covering of aeolian sand that is only about 2 m thick on average. The transition from the one vegetation type to the other at  $16^{\circ} 10' E$ , i.e. from the area with the KOH-0 Aquifer to the area where it is not present, is rapid and takes place within about 200 m. Thus, the good forest growth indicates the presence of aeolian sheet sands of the KOH-0. In areas where the aquifer depth is greater than approximately 15 m, the water is too deep for many trees and tree coverage is less. Two areas where the KOH-0 Aquifer thickness is greater than average are highlighted in Fig. 9. Boreholes in the eastern patch are tightly clustered; the average thickness of the aquifer is 24.5 m and it must have been an area that old, hand-dug wells identified as having rather abundant good water. There is a suggestion that the areas of thicker or thinner sand have a NE–SW elongation but the boreholes are too far apart to be certain of this.

### A 3D map as structural basis for hydrogeological understanding

A consideration of the basic symmetry of depositional sedimentary systems and continuity of lithofacies in space is used to classify the Cubango Megafan into several spatial subsystems in the 3D map. The Namibian part of the megafan forms a half cone. The western section of this has been the focus of this investigation. For area A in Fig. 4, the geophysical logs have made it possible to map an almost complete 3D-distribution of lithofacies units, whereas area B has been compiled from several lithologs but there are insufficient geophysical logs for sound mapping. This area supposedly forms an important transition to area C, the eastern part of the megafan, where a slightly different system is expected due to symmetry considerations. The southern transition to the Oshivelo Aquifers (Bäumle 2004; Bäumle et al. 2001; Margane et al. 2005) is not yet included on the 3D map.

Transitions seen in the megafan are parallel to the contour lines. The 1,115-masl contour line is roughly the line at which water becomes brackish in KOH-2, at least within the range that TEM profiles C, F and D span (Fig. 4). The 1,130-masl contour line represents a transition of eastern megafan facies types to more dominant lake facies types encountered in WW201346. Lithofacies Unit VIII (aeolian sheet sand) that is characteristic for area A vanishes at this elevation. The 1,150-masl line represents the transition of freshwater to brackish water for aquifer KOH-1. TEM sounding C580 represents an important marker where, in the TEM profile C, a high resistivity layer at higher stratigraphic levels vanishes. East of the crest of the megafan, a fluvial system, different from the one that filled the Etosha Depression, is anticipated and a slightly different lithostratigraphy is found, lacking the influence of the palaeolake and of the Kunene Megafan.

### Lithofacies unit distribution and hydrogeology west of the crest of the megafan

The so far best mapped area is area A (Fig. 10a). A total of nine boreholes have geophysical logs deeper than 260 m and end in KOH-2; four of these boreholes reached the bottom of KOH-2. These were used to set up a framework of cross sections for the 3D map. Gamma ray and FEL conductivity logs were compared to lithologs and sections with similar patterns were used to correlate the logs spatially. KOH-2 is characterized by distinctive low gamma and conductivity values (Fig. 6). West of WW201045 and towards the Etosha Depression, KOH-2 becomes brackish. In addition to that, in WW201346 a new and pronounced lithofacies emerges between LU Ib and Ia (Fig. 11). Towards the crest of the megafan, the boundaries of lithofacies are more distinct in the borehole logs. WW201047 shows sharp boundaries between LU I and II, between LU II and IV, and between LU IV and VI. The extent of LU III is more difficult to model. In

WW201045, LU III has a low hydraulic conductivity, elevated gamma ray signals and a sequence of peaks within the conductivity logs. The peaks belong to a stack of alternating clay-rich and sandy layers and are traceable to WW201046 and WW201345. No such peaks are found in the approximate position in WW201047; hence, distinct LU III and LU Ib units could not be resolved (Fig. 11). However, the signal changes in the geophysical logs are more distinct and point to hiatuses above and below KOH-2. In fact, the top of KOH-2 in WW201047 is about 40 m higher than in WW201045. There is a change in inclination of the tops of units LU VIII to LU III and LU II. Two points, perpendicular to the 1,130-masl line, were used to determine the slope of the mapped layers (Fig. 10c). The inclination thus derived is quite similar for the upper layers and lies between 35 and 55 m over a

distance of 100 km. In contrast, the inclination of the top of LU II is greater, being more than 75 m over the same distance, which implies a change in sedimentation of an overlap of different sedimentative systems.

For area A sufficient information was available to calculate 3D-bodies of the lithofacies units and use these to estimate potential volumes of freshwater-bearing groundwater bodies. The area covered by this 3D-map is 4,130 km<sup>2</sup>. Approximately 3,350 km<sup>2</sup> of this are considered to contain freshwater-bearing groundwater bodies. The change from fresh to brackish water lies approximately parallel to the 1,115 masl contour line. Further to the south-east, insufficient data inhibits a clear definition of the transition from saline to brackish water. The groundwater body of KOH-2 is a combination of LU II and LU Ib. Water from LU II contains less fluoride than from LU Ib (Lindenmaier and Christelis 2012)

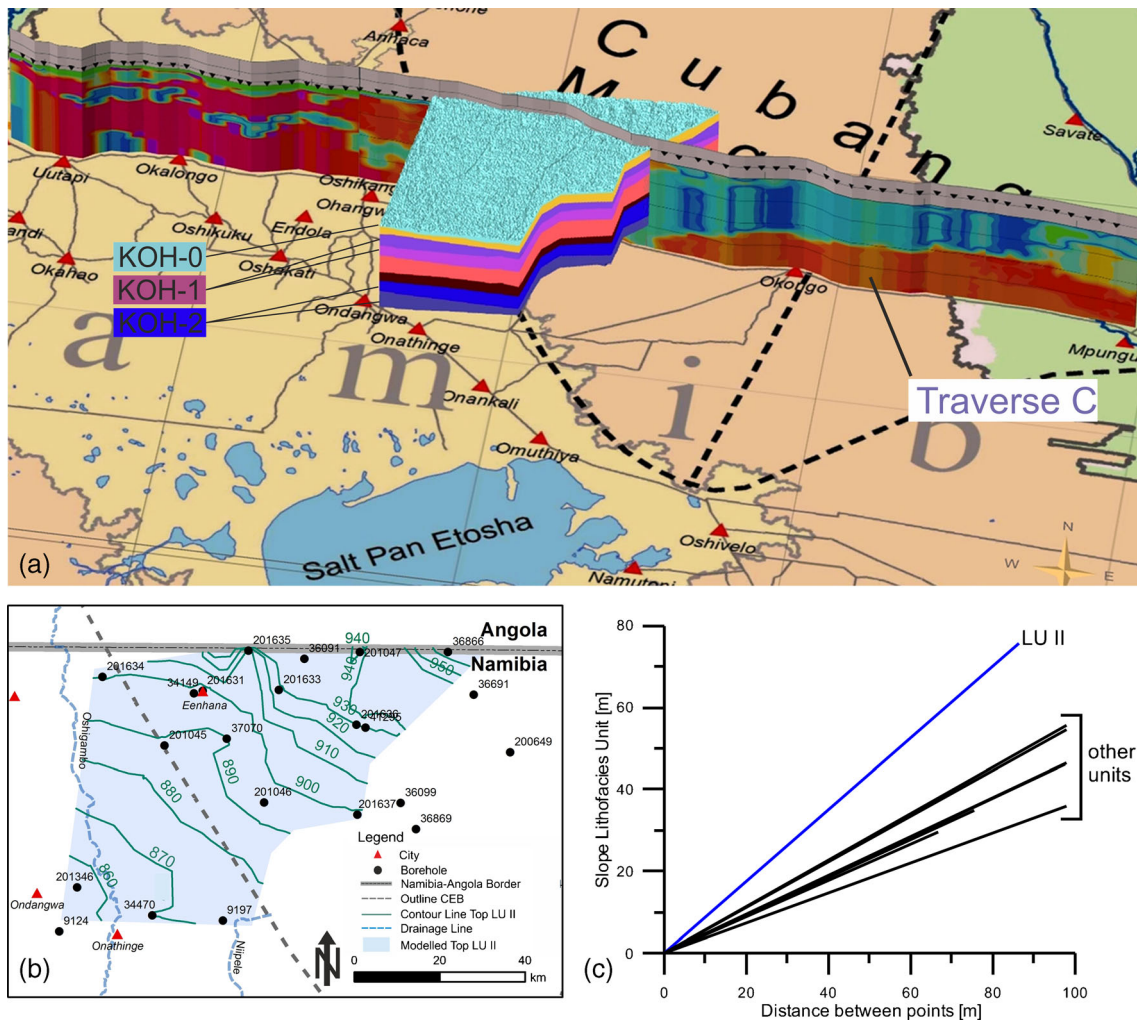


**Fig. 10** a Oblique 3-D map view of lithofacies units of the Cubango Megafan together with the interpretation of the TEM *traverse C* (Figs. 4 and 8). The distribution of *KOH-2* is thought to be well established. *KOH-1*, located within LU V and IV, and *KOH-0* (light blue), need to be resolved in more detail. For the legend of the background map see Figs. 1 and 4. b Isolines of the top of *KOH-2* in masl; the “platform” in the north-eastern edge of the surface is an artefact of the vanishing of LU III and the specific shape of LU distribution in WW201047. c Inclination of tops of lithofacies units between WW201045 and WW201047. The *top of LU II* has a greater inclination than the other tops



which makes it more valuable for exploitation. LU II has a calculated volume of 240 km<sup>3</sup>, and LU Ib has a calculated volume of 134 km<sup>3</sup> and a smaller areal extent than LU II because it does not continue through to borehole WW201047 (Fig. 11). It has to be noted that these are calculated volumes from the 3D map. They do not represent a volume of water; instead, sediments, saltwater and non-extractable water take up a large part of this volume. With the conservative assumptions that an effective porosity of 0.1 prevails and that it will not be possible to extract all the water, a volume of about 5 km<sup>3</sup> of extractable potable water is plausible. The fluoride content is the main concern, besides the possibility of raising salinity if the aquifer is overexploited. The average calculated thickness of LU II is 68 m, the median is 65 m, the minimum is 46 m and the maximum 115 m. The top of LU II lies at an elevation of between 860 and 960 masl (Fig. 10b) that is 200–250 mbgl.

In the mapped area, KOH-1 mainly contains brackish water. No information about the quality of KOH-0 is available; however, the groundwater well database of DWAf (GROWAS I) records a high number of hand-dug wells utilising this aquifer, so that it is assumed to have predominantly freshwater. Calculated volumes for both aquifers are not feasible to use for water-management purposes and a focus on exploration of these aquifers is

needed first. LU VIII has an approximate volume of 30 km<sup>3</sup>.

*Lithofacies unit distribution and hydrogeology eastwards*  
A scientifically sound extrapolation of mapped units from area A towards area B is not feasible. However, for LUs VI–VIII, a few lithologies are available and the geophysical logs of WW200647–WW200649 indicate a continuity of the more surficial layers. Gamma ray and conductivity logs indicate that LU VI contains layers enriched in clay. LU III could extend further east, according to gamma ray and magnetic susceptibility logs, but this needs verification.

Boreholes WW200647–WW200649 which are located along route M111 on an east–west traverse show characteristic sequences of gamma ray and conductivity logs that are used for lithofacies unit identification (Fig. 12). In WW200649, LU VII shows a sharp rise in conductivity and then a gradual decline with increasing depth. A similar profile is observed in LU VI which is continuous into LU V; however, the gamma ray response is low in most of LU VI and low in LU V. This double sequence is typical for several borehole logs. A significant rise of the gamma ray signal occurs in a lens in LU IV. It is traceable to WW201047 but more detailed sedimentological analyses are needed. Van Wyk (2009a) describes

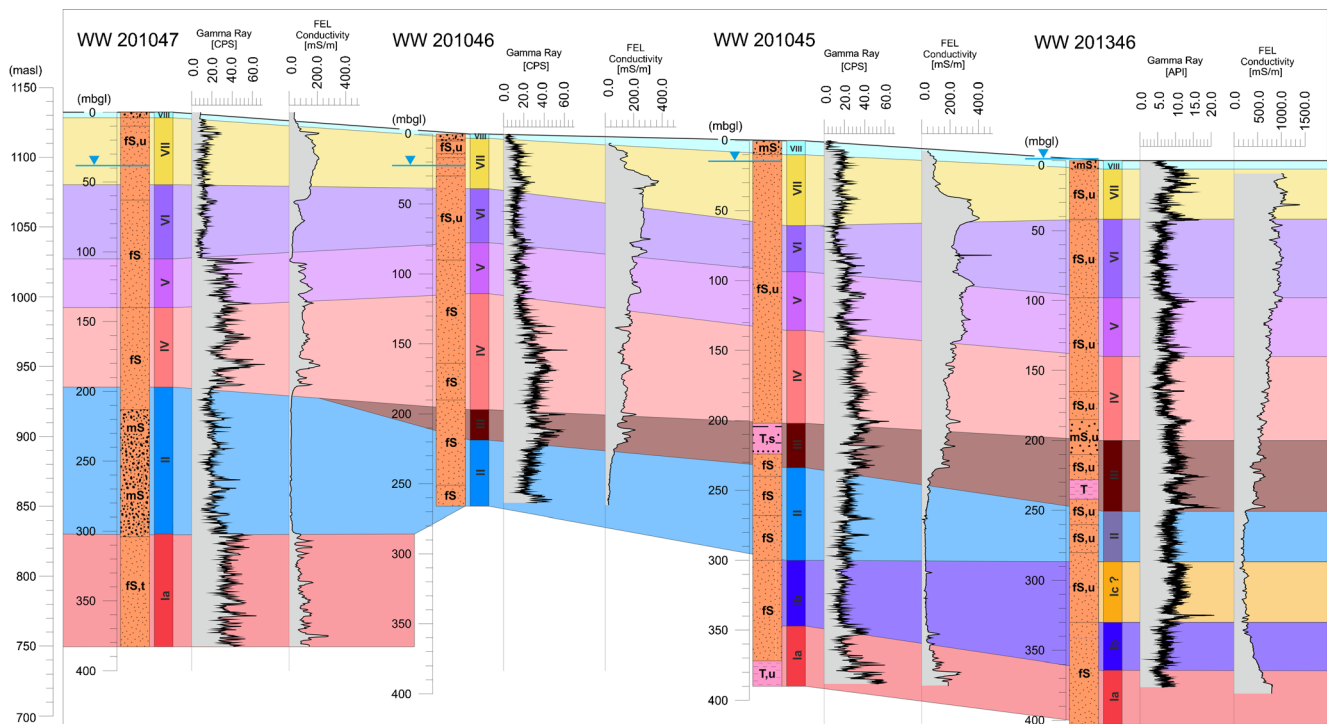


**Fig. 11** Profile constructed from WW201047 (proximal) to WW201346 (distal) down the Cubango Megafan with WW201045 and WW201046 projected onto this profile (see Fig. 3 for the location of boreholes). Existence of LU III in WW201047 is not clear. Principally, top and base of LU II in WW201047 seems to be raised in relation to other boreholes. In WW201346, an additional layer occurs between LU II and LU Ib. Note that geophysical logs of WW201346 were conducted with different probes. Colours of respective LUs match with Figs. 10a and 12

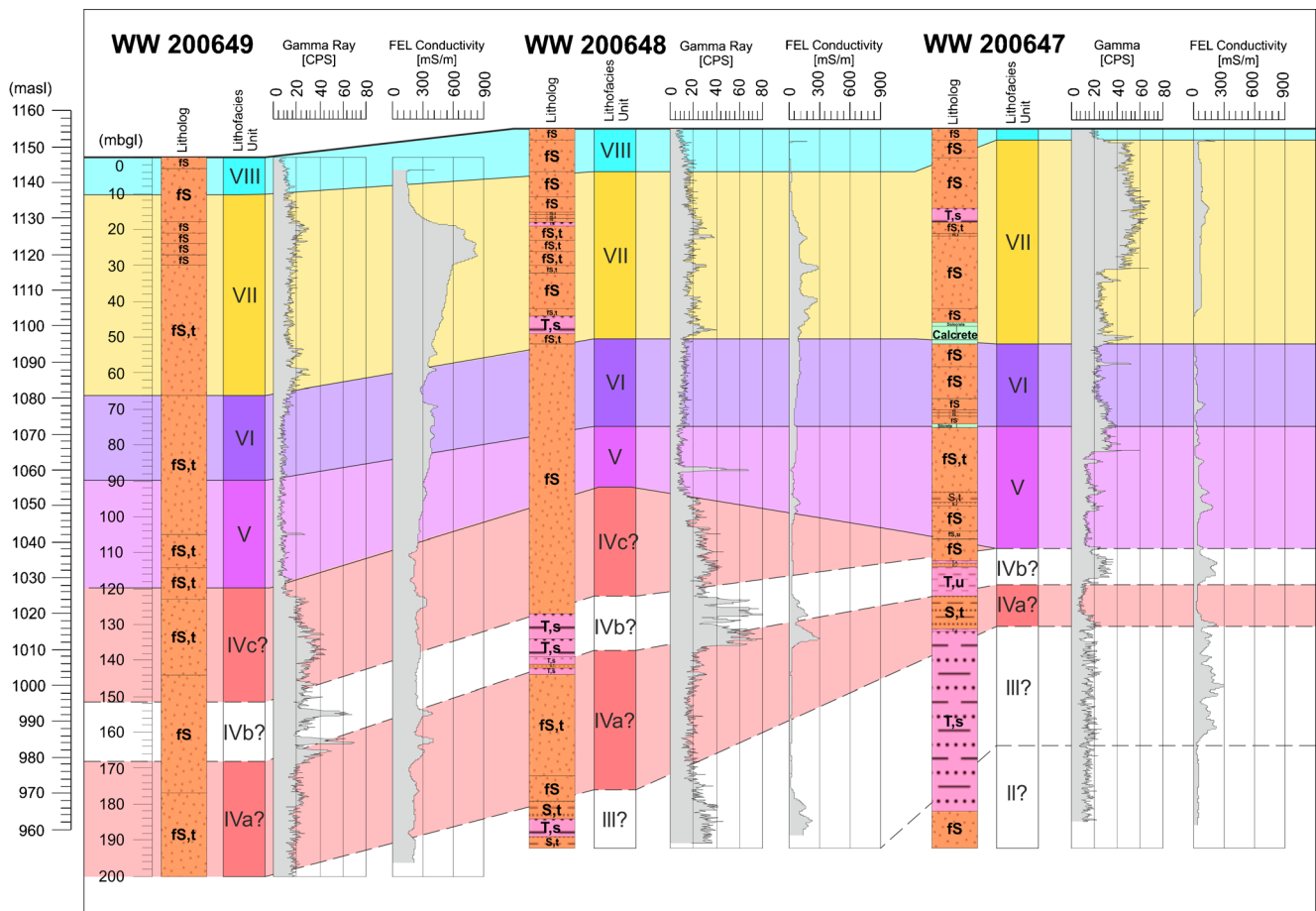


**Fig. 12** Cross section from WW200649 to WW200647; the gamma ray and conductivity logs of WW200647 were taken during a different logging campaign with different probes. Below LU *V*, correlation is uncertain. Colours of respective LUs match with Figs. 10a and 11

33 boreholes in areas A and B and states that, at a depth below approximately 70 mbgl, better sorting of sediments results in more conductive layers which matches with the geophysical logs. Yields increase from west to east but are generally low (2–4 m<sup>3</sup>/h) compared to KOH-2 (16 m<sup>3</sup>/h). More geophysical logs would greatly enhance the mapping in areas B and C.

## Discussion

Sedimentary basins like the Owambo Basin and particularly the Cubango Megafan with its predominance of sandy sediments are extremely difficult to interpret, particularly when there is so little that is visible by non-invasive exploration methods. The nature of a low-gradient, low-sinuosity losimean megafan (Stanistreet and McCarthy 1992) which has been built up under seasonal climatic conditions makes such a feature difficult to recognise and the sedimentary environment under which it formed particularly difficult to unravel. Many previous authors who have worked on the Kalahari (Buch 1997; Buch and Rose 1996; Moore 1999; Moore and Larkin 2001; Goudie 2005; Haddon and McCarthy 2005) did not recognise this megafan. It is only recently that this

almost invisible megafan was brought to the awareness of scientists (Wilkinson et al. 2006) and (Miller et al. 2010; Wilkinson et al. 2009). Its recognition and an understanding of how it formed will be a major step in understanding how sediments accumulated in the Kalahari Basin. Other Kalahari fans and megafans will undoubtedly be found within the basin and they too could have the potential for deep, potable groundwater reservoirs.

Little is known about the depositional environment of the early Kalahari succession in the CEB. Figure 13 illustrates possible erosional and depositional zones within the Owambo Basin. The Late Cretaceous may have seen the first limited sediment accumulation within the basin. This began to increase during the Oligocene (Fig. 13a). Erosion occurred mainly in the Angolan Highlands. These highlands are dominated by metamorphic or granitic rocks, while Damaran limestones, dolomites and argillaceous carbonates are found in the western and southern mountains, but the ~50-m thick, clay-rich, Africa-wide regolith produced under the hot-house climatic conditions of the Cretaceous African Erosion Cycle (Burke and Gunnell 2008; Miller 2008) had to be removed first. Thus, the basal red sediments in the Owambo Basin, the Ombalantu Formation, are very clay rich (Miller 1997, 2008) and are considered as a basal aquitard. Much of the

initial deposition would have been around the basin margins, particularly in the north in the regions of the greatest sediment supply. It is assumed that the Cubango (Okavango) and Kunene valley systems were not yet developed and deposition took place along a broad southerly swath into the Owambo Basin (Fig. 13a). With time, deeper erosion in the highlands began to supply more quartz-rich sediments. Uplift of the highlands exposed the apron of basal Kalahari sediment around them, these being more proximal and consequently more quartz rich than the sediments further into the basin. Erosion and reworking of this apron provided an additional quartz-rich component to the sediments higher up in the Kalahari succession. As depositional conditions changed from oxidising to reducing, the red beds of the

lower Kalahari succession gave way to the white sands and green clays of the Andoni Formation (Miller 2008; Miller et al. 2010). The Damaran carbonates in the west could have been the main source of the clays in the Kunene Megafan; however, composition of clays also suggest a volcanic part. The uplift initiated the development of a two-fold drainage system (Fig. 13b) and possibly, at the time that depositional conditions changed from oxidising to reducing, the Cubango and Kunene Megafans began to develop. The shape of the Cubango Megafan indicates that the outlet to the east, if there ever was one, became clogged with sediments and vanished.

With continuing uplift and eastward erosion of the Great Escarpment, the catchment of the Kunene loses more area than the catchment of the Okavango. This is

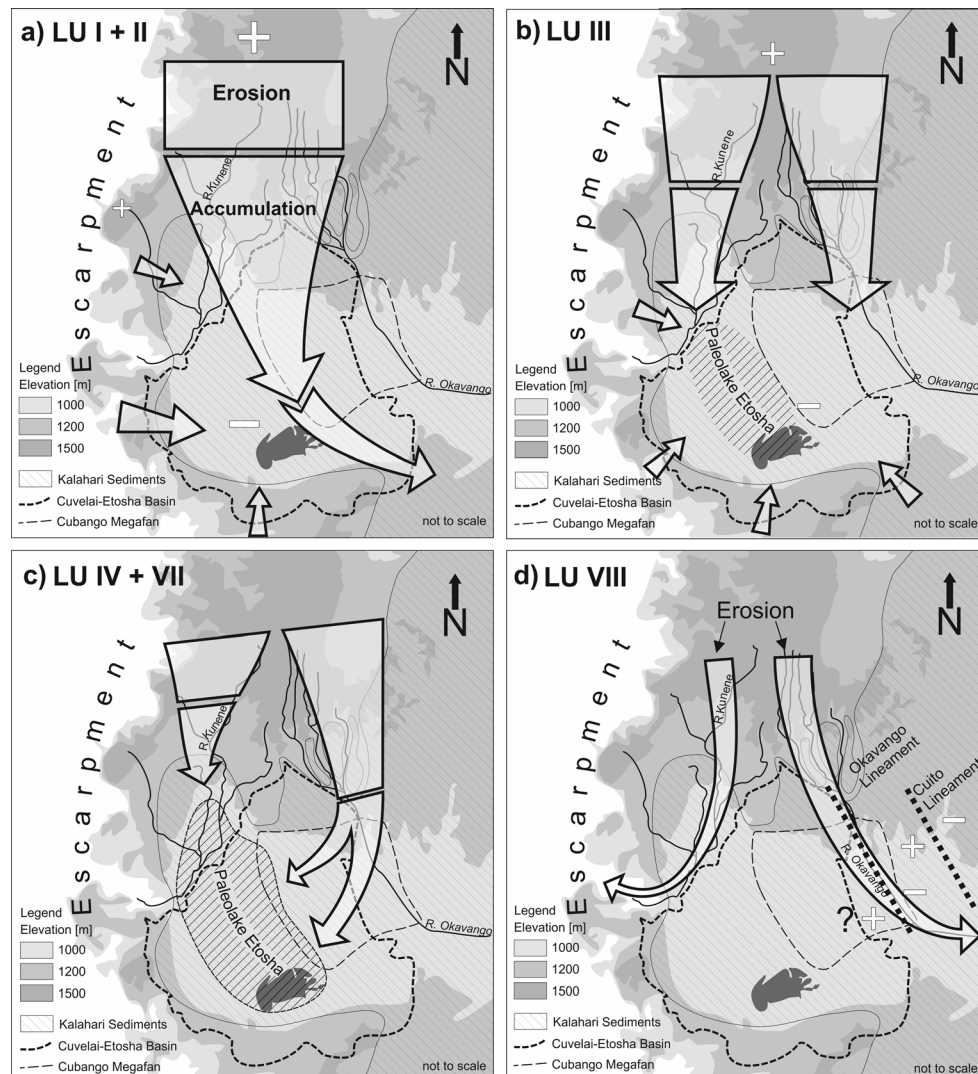


**Fig. 13** Flow evolution in the Cuvelai-Etoshia Basin: possible erosion and deposition zones within the Owambo Basin from the Late Cretaceous–Palaeocene to Recent. **a** Sediment was mainly supplied over a broad swath from the north; neither the Kunene nor the Okavango were established. There may have been outflow to the east. Small-scale catchments delivered sediments from the west. **b** The palaeo Kunene and Okavango systems became established. Uplift of the Angolan highlands facilitated reworking of older Kalahari sediments. **c** Continued build-up of the Kunene and Cubango Megafans with the latter dominant; termination in a common end point, Palaeolake Etosha. **d** Return of a more humid climate after the desert conditions of the upper Pliocene: capture of the upper Kunene by the lower Kunene and diversion of Okavango to the east

illustrated as a decline in the volume of sediment supply from the Kunene relative to the Cubango Megafan (Fig. 13c). Sediments that form the two systems interfinger at the margins of the two megafans and the final contribution of sediment into the realm of the Cubango Megafan at the location of borehole WW201045 is at the top of LU V where the last of the north-western “mandarin garnets” was described (Dill et al. 2012). Both Kunene and Okavango systems fed their waters into the terminal lake, Palaeolake Etosha, with increasing dominance of the Okavango and its delta. The lake level may have varied in response to climate variability. Periodic expansion of the lake or the development of a series of linked lakes took place during more humid periods in a north-westerly direction where the supply of sediment was less and more clay rich.

Finally, arid conditions slowly set in and the flow of the Okavango and Kunene via their respective megafans into Palaeolake Etosha eventually dried up completely (Miller et al. 2010). Desert conditions became fully developed during global cooling as a result of the rapid growth of the Arctic ice cap some 2.67 million years ago during the upper Pliocene (Berner and Streif 2004). Once a more amenable climate returned and rainfall increased, possibly about 1 million years ago (Miller et al. 2010), the lower Kunene captured the upper Kunene (Wellington 1938) and flow in the Okavango River started to cut a new, fault-controlled, south-south-easterly flowing channel into the eastern flank of its old megafan (Fig. 13d), both probably tectonically induced. Parallel lineaments/faults control the flow of the Okavango, Cuito and Zambezi rivers (Mendelsohn et al. 2010) south of the Angolan Highlands. The incision of the Okavango into its own delta is now more than 50 m. The various cements in the sands of the Cubango Megafan shed light on the palaeo-climatological boundary conditions and the palaeo-hydraulic systems that prevailed during and after deposition (Dill et al. 2012).

The tectonic impact on the evolution of the Owambo basin is not yet considered in its full extent. The valleys of eastern tributaries of the Okavango show that uplift is to the east while the Okavango itself must be located on a fault (Fig. 2c–d). Neogene Kalahari sediments west of the Kunene (Fig. 1b) build up an east-dipping ramp that indicates tectonic activity of the escarpment and a possible fault in the northern Kunene Valley. An attempt to understand the tectonic setting by geophysical exploration would greatly help to improve knowledge of the groundwater systems.

The investigations to date have shown that there is potential for high-quality groundwater resources within the Cubango Megafan. Filling gaps in the understanding of the subsurface is essential following the lateral extent of the aquifers and for effective, long-term management of them. We are still a long way from an adequate understanding of the hydrogeology and sedimentology of the Cubango Megafan and the Cuvelai-Etosha Basin as a whole.

However, exploring this system showed that the search for groundwater might need a greater effort beyond the

limits of a standard hydrogeological exploration. Searching for the aquifers also required an understanding of the sedimentological system, which explains some specific characteristics of aquitards and aquifers, e.g. the smectite and silicate gels as confining units or the discrepancy of low clay contents and still highly confining layers due to the filling of pores with smectite. In fact, the need for drinkable water in Africa should lead to exploration strategies with extent and methods that are used in oil exploration.

Quantitative and qualitative descriptions of the three aquifers need much more data on the distribution of subsurface stratigraphic units and about the sedimentological environment under which they formed. So far, area A is considered to be well explored but spans just about 7 % of the total extent of the Cubango Megafan with an approximate size of 55,000 km<sup>2</sup>. LU III is critical as the confining layer to the KOH-2 aquifer. Its clay content makes it readily recognisable in lithologs and geophysical logs and, therefore, readily mappable with borehole geophysics. However, its extension east of area A is still uncertain and information on its total lateral extent would provide essential answers about the spatial and temporal evolution of the basin and possible recharge areas. Also, the groundwater resources availability could be increased with further exploration of KOH-2 towards the east. The 3D-mapping attempt greatly helped to order the sparse information available according to its significance and to build up a plausible hydrogeological concept that also is able to be brought to the public.

The question of whether fossil or rechargeable resources were found is yet unanswered. Samples for C14-age determination were taken and analysed from deep-seated groundwater wells. Ages of 10,000–30,000 years were determined but data are unreliable due to the unknown construction of wells and screen position. It is assumed that a slow recharge has been ongoing since aridity diminished about 1 million years ago and that a saltwater aquifer was slowly refreshed. However, as long as recharge paths and quantities of recharge are not precisely determined, water managers have to accept that fossil resources were found and these need to be handled with care. Exploration of the aquifer is ongoing, focussing on hydrochemical investigation and age determination, as well as numerical modelling.

Three major recharge paths for the deep-seated KOH-2 aquifer are determined; these are closely linked to the sedimentary development of the CEB and Cubango Megafan. The first recharge path considered is a top-down recharge through geological windows to the north or east of area A. In support of this is the continuous freshwater zone recorded by the TEM soundings (Fig. 8, east of Okongo). However, the TEM soundings are possibly not able to resolve confining layers in this section and most of the KOH-1 seems to be confined (Van Wyk 2009a). The role of smectite and silica gels as confining elements is still quite unknown and they were not detected with TEM sounding or borehole logging. In addition, the geophysical borehole logs of WW200647–WW200649

show also layers enriched in clay. Pump tests in KOH-1 aquifers show low yields so that vertical recharge would be considered to be rather limited.

A second recharge path would be regional lateral discharge from recharge areas in the Angolan Highlands. North of the megafan, older Neogene sediments crop out and are cut by the Okavango (Fig. 1b). These could be equivalents of lithofacies units like LU II and function as a recharge zone. In addition, the highlands are subject to higher yearly precipitation. Travel times for waters from these recharge zones to the southern tip of the megafan would inhibit a quick recharge.

A final possibility for recharge of KOH-2 is from the Okavango River itself which has incised deeply into its former megafan. River bank infiltration is a distinct possibility in view of the fact that the water level in the river is almost identical to rest water levels in the KOH-2 aquifer. Extrapolation of LUs to the Okavango show that LU V and VI would theoretically intersect the river.

The major recharge process remains yet unknown but research and development on the Cubango Megafan is ongoing. Further field investigation needs to focus on (1) exploratory and especially cored boreholes east of the mapped section in the direction toward the Okavango River, (2) investigation of river-sediment interaction there, and (3) an expansion of exploration northwards towards the Angolan Highlands.

**Acknowledgements** Drilling was enabled by funds of the European Union and the German Federal Ministry for Economic Cooperation and Development. The research has been funded by the Federal Institute for Geosciences and Natural Resources. The authors want to thank DWAF and the DWAF-BGR-project for providing data, samples for mineralogical and sedimentological investigation and field support. Uli Gersdorf and Mariola Kosenko are thanked for their graphical support and Gabi Hartmann for ArcGIS artwork. Many others that initiated and supported the exploration of the aquifers are especially thanked for their contributions. Lastly, I would like to thank the three reviewers for their helpful comments and positive response.

## References

- Bäumle R (2004) Groundwater investigations of the Oshivelo artesian aquifer: isotope sampling campaign for the investigation of the recharge, groundwater quality and flow mechanisms. Report, IAEA/DWA, Windhoek, Namibia
- Bäumle R, Himmelsbach T, Bufler R (2001) Conceptual hydrogeological models to assess the groundwater resources of the heterogeneous fractured aquifers at Tsumeb (northern Namibia). In: Seiler K-P, Wohnlich S (eds) Proc. of the XXXI IAH Congress: new approaches characterizing groundwater flow, Munich, 10–14 September 2001. Balkema, Lisse, The Netherlands, pp 245–249
- Berner U, Streif H (2004) Klimafakten: der Rückblick—ein Schlüssel für die Zukunft [Facts about climate: retrospect—a key to the future]. Bundesanstalt für Geowissenschaften und Rohstoffe, Hanover, Germany
- Bittner ACW (1998) Drilling of a deep freshwater borehole in the Eenhana area applying the EDL-Technique. Ministry of Agriculture Ward, Dept. of Water Affairs, Windhoek, Namibia, 12 pp
- Bittner ACW (2008) Drilling and testing of 4 exploration wells along M110 between Mpungu and Elundu. Bittner Water Consult, Windhoek, Namibia, 41 pp
- Bittner ACW, Kleczar ML (2006) Desk study report: Cuvelai-Etosha groundwater investigation. Dept. of Water Affairs and Forestry, Bittner Water Consult, Windhoek, Namibia
- Buch MW (1997) Etosha Pan: the third largest lake in the world? *Modoqua* 20:49–64
- Buch MW, Rose D (1996) Mineralogy and geochemistry of the sediments of the Etosha Pan region in northern Namibia: a reconstruction of the depositional environment. *J Afr Earth Sci* 22:355–378
- Buch MW, Trippner C (1997) Overview of the geological and geomorphological evolution of the Etosha region, northern Namibia. *Modoqua* 20:65–74
- Burke K, Gunnell Y (2008) The African erosion surface: a continental-scale synthesis of geomorphology, tectonics, and environmental change over the past 180 Million years, vol 201. Geological Society of America, Boulder, CO
- Christelis G, Struckmeier W (2001) Groundwater in Namibia: an explanation to the hydrogeological map of Namibia. John Meinert, Windhoek, Namibia
- de Araújo AG, Perevalov OV, Jukov RA (1988) Carta geológica de Angola [Geological map of Angola]. Instituto Nacional de Geologia de Angola, Luanda, Angola, Scale: 1:1,000,000
- Dill H, Kaufhold S, Lindenmaier F, Dohrmann R, Ludwig RR, Botz R (2012) Joint clay-heavy-light mineral analysis: a tool to investigate the hydrographic-hydraulic regime of Late Cenozoic deltaic inland fans under changing climatic conditions (Cuvelai-Etosha Basin, Namibia). *Int J Earth Sci*. doi:10.1007/s00531-012-0770-7
- DIN 18130-1 (1998) Baugrund: Untersuchung von Bodenproben; Bestimmung des Wasserdurchlässigkeitsbeiwerts—Teil 1, Laborversuche [Soil, investigation and testing: determination of the coefficient of water permeability—part 1, laboratory tests). Deutsches Institut für Normung, Hanover, Germany
- Fenner J (2010) Silt fraction analysis of the boreholes NAM 201216 and 201217, Namibia and its indications for palaeoenvironment and sediment age: a pilot study. Bundesanstalt für Geowissenschaften und Rohstoffe, Hanover, Germany, 27 pp
- Fenner J, DiStefano A (2004) Late Quaternary oceanic fronts along Chatham Rise indicated by phytoplankton assemblages, and refined calcareous nannofossil stratigraphy for the mid-latitude SW Pacific. *Mar Geol* 205:59–86
- Fielitz K, Stadler C, Schildknecht F (2004) Results of time domain electromagnetic soundings and direct current soundings for groundwater exploration in three regions of NE Namibia. Bundesanstalt für Geowissenschaften und Rohstoffe, Hanover, Germany
- Garstang M, Ellery TS, McCarthy TS, Scholes MC, Scholes RJ, Swap RJ, Tyson PD (1989) The contribution of aerosol- and water-borne nutrients to the functioning of the Okavango Delta ecosystem, Botswana. *S Afr J Sci* 94:223–229
- Goudie AS (2005) The drainage of Africa since the Cretaceous. *Geomorphology* 67:437–456
- Haddon IG (2005) The sub-Kalahari geology and tectonic evolution of the Kalahari Basin, southern Africa. University of Witwatersrand, Johannesburg
- Haddon IG, McCarthy TS (2005) The Mesozoic-Cenozoic Interior sag basins of Central Africa: the Late-Cretaceous-Cenozoic Kalahari and Okavango basins. *J Afr Earth Sci* 43:316–333
- Hecky RE, Kilham P (1973) Diatoms in alkaline, saline lakes: ecology and geochemical implications. *Limnol Oceanogr* 18:53–71
- Hedberg RM (1979) Stratigraphy of the Owamboland Basin, South West Africa. University of Cape Town, Dept. of Geology, Cape Town, South Africa
- Lindenmaier F, Christelis G (eds) (2012) Groundwater for the north of Namibia: summary report of activities of phase I—exploration of Ohangwena II Aquifer and preliminary isotope study, vol Ia. Bundesanstalt für Geowissenschaften und Rohstoffe, Hanover, Germany, 64 pp

- Lindenmaier F, Fenner J, Gersdorf U, Kaufhold S, Kringel R, Lohe C, Ludwig RR, Nick A, Noell U, Quinger M, Schildknecht F, Walzer A (2012) Groundwater for the north of Namibia, vol Ib. Kalahari Research Project: results of analysis from drill holes on the Cubango Megafan. Bundesanstalt für Geowissenschaften und Rohstoffe, Hanover, Germany, 50 pp
- Margane A, Bäumle R, Schildknecht F, Wierenga A (2005) Groundwater Investigations in the Oshivelo Region. Main hydrogeological report, vol IVGW11, BGR, Hanover, Germany, 207 pp
- Martin H (1950) Südwestafrika [South-west Africa]. *Geol Rundsch* 38:6–14
- Mathers SJ, Wood B, Kessler H (2011) GSI3D software manual and methodology. BGS internal report OR/11/020, British Geological Survey, Keyworth, UK, 152 pp
- McCarthy TS, Ellery WN, Rogers KH, Cairncross B, Ellery K (1986) The role of sedimentation and plant growth in changing flow patterns in the Okavango Delta. *S Afr J Sci* 82:579–584
- McCarthy TS, Stanistreet IG, Cairncross B (1991) The sedimentary dynamics of active fluvial channels on the Okavango fan, Botswana. *Sedimentology* 38:471–487
- Mendelsohn J, El Obeid S, Roberts G (2000) A profile of north-central Namibia. Gamsberg Macmillan, Windhoek, Namibia
- Mendelsohn JM, van der Post C, Ramberg L, Murray-Hudson M, Wolski P, Mosepele K (2010) Okavango Delta: floods of life. RAISON (Research and Information Services of Namibia) for IUCN and HOORC, Windhoek, Namibia
- METI and NASA (2011) ASTER GDEM version 2, release 17.10.2011. <http://asterweb.jpl.nasa.gov/gdem.asp>. Accessed 9 April 2013
- Miller RMG (1997) The Owambo Basin of northern Namibia. In: Selly RC (ed) *Sedimentary basins of the world: African basins*. Elsevier, Amsterdam, pp 237–268
- Miller RMcG (2008) The geology of Namibia, vol 3: Palaeozoic to Cenozoic. Ministry of Mines and Energy, Geological Survey, Windhoek, Namibia
- Miller RMcG (2010) Lithology of boreholes WW 201216 and WW 201217, Ohangwena region, Namibia. Dept. of Water Affairs and Forestry, Windhoek, Namibia
- Miller RMcG (2013) Groundwater for the north of Namibia: technical Note no. 1—drill-log interpretation and evaluation of drillings KOH I and KOH II aquifers, Ohangwena Region, Cuvelai-Etoshia Basin. BGR report 05-2345, DWAF, Windhoek, Namibia and BGR, Hanover, Germany
- Miller RMcG, Schalk KEL (1980) Geological map of Namibia 1:1,000,000. Geological Survey of Namibia, Windhoek, Namibia
- Miller RMG, Pickford M, Senut B (2010) The geology, palaeontology and evolution of the Etosha Pan, Namibia: implications for terminal Kalahari deposition. *S Afr J Geol* 113:307–334
- Milzow JC (2008) Hydrological and sedimentological modelling of the Okavango Delta wetlands. ETH Zurich, Zurich, Switzerland
- Milzow JC, Kgotlhang L, Bauer-Gottwein P, Meier P, Kinzelbach W (2009) Regional review: the hydrology of the Okavango Delta, Botswana: processes, data and modelling. *Hydrogeol J* 17:1297–1328. doi:10.1007/s10040-009-0436-0
- Moore AE (1999) A reappraisal of epeirogenic flexure axes in southern Africa. *S Afr J Geol* 102:363–376
- Moore AE, Blenkinsop T (2002) The role of mantle plumes in the development of continental scale drainage patterns: the southern African example revisited. *S Afr J Geol* 105:353–360
- Moore AE, Larkin PA (2001) Drainage evolution in south central Africa since the breakup of Gondwana. *S Afr J Geol* 104:47–68
- Pielawa J, Rehli HJ, Röttger B, Sengpiel K-P, Siemon B, Voss W (1995) The BGR Geophysical Helicopter Survey in the eastern Owambo Area, 1993. Technical report, BGR, Hanover, Germany
- Preuss H, Vinken R, Voss HH, Barckhausen J, Beckmann A, Hennig E-W, Hinze C, Hohmann HH, Reuter G (1991) Symbolschlüssel Geologie. Niedersächsisches Landesamt für Bodenforschung und BGR, Hanover, Germany
- Schildknecht F (2012) Groundwater for the north of Namibia: groundwater exploration with TEM soundings in the Cuvelai-Etoshia-Basin, vol Id. Bundesanstalt für Geowissenschaften und Rohstoffe, Hanover, Germany, 222 pp
- Sobisch H-G (2014) Insight Geologische Software Systeme GmbH, Cologne, Germany. <http://subsurfaceviewer.com>. Accessed 23 April 2014
- Stanistreet IG, McCarthy TS (1992) The Okavango Fan and the classification of subaerial fan systems. *Sediment Geol* 85:115–133
- Thomas DSG, Shaw PA (1990) The Kalahari environment. Cambridge University Press, Cambridge
- Van Wyk B (2009a) Drilling report for three deep boreholes in the Cuvelai-Etoshia Basin. Dept. of Water Affairs and Forestry, Windhoek, Namibia, 71 pp
- Van Wyk B (2009b) Rural Water Supply Drilling Program 2009: Ohangwena Region. Bittner Water Consult, Windhoek, Namibia, 18 pp
- Verissimo LM (2005) Plano de urbanizacao da cidade de Ondjiva: caracterizacao biofisica. Offices of Studies, Planning and Statistics, Ondjiva, Angola. Available at <http://bibliotecaterra.angonet.org/node/360>. Cited 23 April 2014
- Walzer A (2010) Multilayered aquifers in the central-north of Namibia and their potential use for water supply. Technische Universität Dresden, Dresden; Bundesanstalt für Geowissenschaften und Rohstoffe, Hanover, Germany, 114 pp
- Wellington JE (1938) The Kunene River and the Etosha Plain. *S Afr Geogr J* 20:150
- Wilkinson MJ, Marshall LG, Lundberg JG (2006) River behaviour on megafans and potential influences on diversification and distribution of aquatic organisms. *J S Am Earth Sci* 21:151–172
- Wilkinson MJ, Miller RM, Allen CC, Kreslavsky MH, Eckardt F (2009) Megafans as hydrous environments. Workshop on Modeling Martian Hydrous Environments Lunar and Planetary Institute, Houston, TX, June 2009